Synthesis and physical properties of nickel nanoparticles and Ni/SiO_2 Core/Shell structure

A dissertation submitted to The University of Manchester for the degree of

Master of Science by Research in the Faculty of Engineering and Physical Science

Hanan Alchaghouri

2010

School of Chemistry

Table of Contents

List of Figures

Declaratin

I, Hanan Alchaghouri, confirm that this work submitted for assessment is my own and is expressed in my own words. Any uses made within it of the works of other authors in any form (e.g. ideas, figures, text, tables) are properly acknowledged at the point of their use. A full list of the references employed has been included.

No portion of the work referred to in this dissertation entitled “Synthesis and physical properties of nickel nanoparticles and Ni/SiO_2 core/shell structure" has been submitted in support to any application for another degree or qualification at this or any other university or other institute of learning.

Acknowledgements

In order to achieve any aims in life, help, advice, suggestions, patience, and support are required, either directly or indirectly, and this can be provided by a variety of people. I take this opportunity to mention a few of them, and extend my sincere thanks to everyone who has played a role in assisting me in achieving this degree.

First and foremost, I am extremely grateful to Damascus University, with particular mention to Dr. Malak Aljouba for giving me the chance to study at The University of Manchester.

I would like to thank Dr. John Thomas for guiding and helping me; materials technical staff: Michael Faulkner, Judith Shackleton and Alan Harvey for all their help in SEM, XRD and TEM; Chemistry administration staff, particularly Lorraine Onabanjo; all my group members for all their help: Alexander Lockett, Gemma Stansfield, Enteisar Albrasi. My friend Fatima Alsadi and her husband.

I also extend heartfelt thanks to my parents for their constant support and love.

Abstract

Magnetic nanoparticles with critical size below 10-20 nm currently attract attention as they have distinctive properties such as a large magnetic moment and behave like giant paramagnetic atoms with a fast response to applied magnetic fields with negligible remanence and coercivity. In addition, they have a single magnetic domain and show superparamagnetic behaviour with blocking temperature. These characteristics make superparamagnetic nanoparticles possess significant applications in biomedical fields. However, nanoparticles need to be protected to be stable and avoid the loss of their magnetism. This can be accomplished by coating nanoparticles with organic species or with an inorganic layer, such as silica. The protecting shells not only stabilise the nanoparticles, but can also be used for further functions. This work presents experimental results on the preparation of fine Ni/NiO nanoparticles via a reduction method. The nanoparticles were prepared by reducing nickel-acetate with 1-propanol in the presence of Pd seeds and polyvinylpyrrolidone (PVP) as a stabiliser. The nanoparticles were further coated with silica (SiO_2) by hydrolysis of tetraethyl orthosilicate (TEOS) in 2-propanol, both with and without a primer (gelatine). The effect of reaction conditions on coating was studied. The nature and characteristics of the Ni nanoparticles and Ni/SiO_2 were studied by a number of techniques such as Scanning Electron Microscopy (SEM), X-Ray Diffraction (XRD), Transmission electron microscopy (TEM), energy-dispersive x-ray spectroscopy (EDX) and Fourier Transform-Infrared Spectroscopy (FTIR). The magnetic measurements of Ni nanoparticles was performed by using superconducting quantum interference device (SQUID) magnetometer.

Finally, an overview of the project is presented and techniques that have been used to characterise nanoparticles. The experimental is outlined in chapter 4.

1 INTRODUCTION

1.1 Introduction

Nanoparticles are the most important class in nanotechnology. They are zero dimensional nano-scale (one billionth of a meter, 10^{-9}m) materials [1].Such materials exhibit chemical and physical properties significantly different from bulk particles [2] due to their size [1]. For example, the gold nanoparticles have a different colour (red) and melting point (approximately 300 ℃ for 2.5 nm size) in comparison with ordinary ones(1064 ℃) [3]. In addition, the atomic and electronic characteristics of fine nanoparticles differ from bulk materials.

Magnetic Nanoparticles have a widespread applications in different fields including chemical, energy, electronics and biomedical applications such as magnetic resonance contrast media and therapeutic agents in cancer treatment. This is dependant to their unique size and shape; this relates to their physical, chemical, magnetic and active large surface properties. Therefore, much attention has been paid for synthesizing and studying the properties of magnetic nanoparticles. There are lots of methods which were used to produce these particles such as chemical reduction, microemulsion and thermal decomposition [1, 4, 5]. The challenge is to produce stable and uniform particles with critical size [6]. Recently, there has been an effort to develop new technologies for coating and controlling the size, shape and surface of magnetic nanoparticles [4, 5].

In this work, we tried to synthesise Ni nanaoparticles with critical size and coated them with uniform Silica layers and studied their physical properties.

1.1 Magnetic properties of nanoparticles

The magnetic response of a material is classified into five types: diamagnetic, paramagnetic, ferromagnetic, antiferromagnetic and ferrimagnetic (see Fig.1).

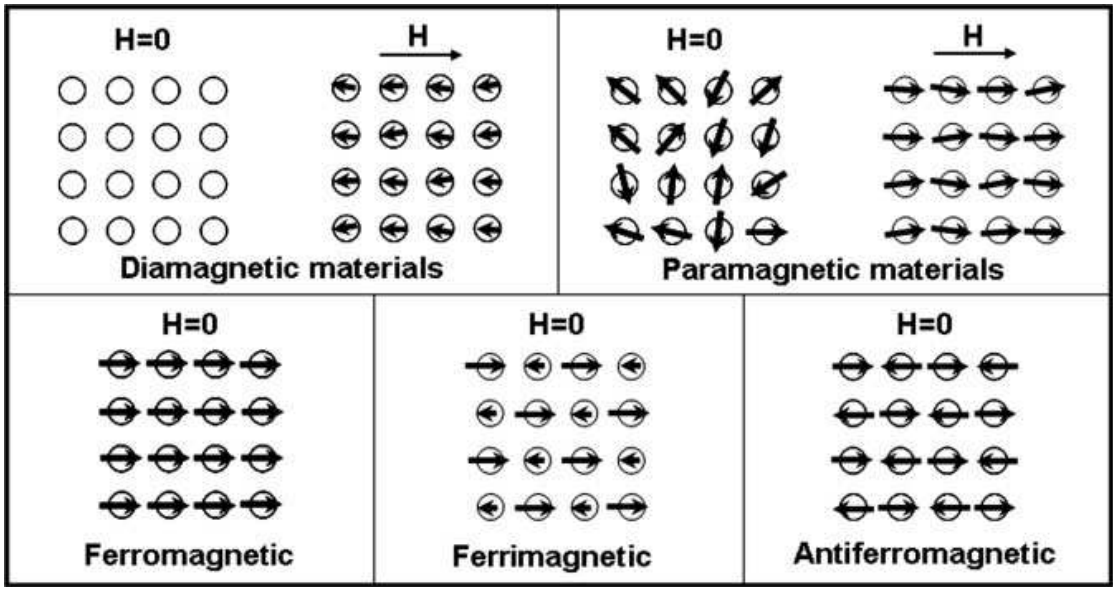

Figure1 :The types of magnetism of materials [7].

This division depends on response these materials to externally applied magnetic field. Diamagnetism is very weak property with negative susceptibility ($\chi < 0$). This phenomenon causes a weak repulsion for the subshells which are filled with paired and opposite magnetic moments. The electron's orbital motion in this state is in the opposite direction to applied field. The other forms of magnetic properties are partially attributed to unpaired electrons in atomic shells. Paramagnets have a small positive magnetic susceptibility ($\chi \approx 0$). It causes in the materials possessing a random dipoles moment, to be aligned in parallel in the presence of applied field. Paramagnetism is stronger than diamagnetism, varies inversely with temperature. Some paramagnetic materials exhibit ferromagnetism below the Curie temperature. Ferromagnetism is a permanent magnetisation that exhibits a long-range ordering phenomenon at the atomic level where atomic magnetic moments line up in the in the absence of an applied field in the domain region. While in anti-ferromagnetism, the dipoles of equal magnitude are arranged in an anti-parallel configuration. The magnetism

converts to paramagnetism above the Neel temperature (NT). In a ferrimagnet unequal magnitude moments line up parallel in the same direction and others antiparallel.

1.1.1 Effects of size and surface on the magnetism of nanoparticles

The magnetic properties of nanoparticles are affected by the size of the system as well as its surface [8]. The Size effects were first discovered in the materials ranging in size 10-100 nm which called 'fine particles' [1]. The finite size which due to the effect of electrons quantum confinement has much attraction related to their single domain nature [8]. The domain feature of the magnetic properties of nanoparticles is superparamagnetic which is the most important limits for the finite size effects [5]. A lots of research are studied to overcome superparamagnetic limit, one of this methods is by exchange bias by using ferromagnetic (core)/antiferromagnetic (shell) systems [9].

When the diameter of ferro- or ferrimagnetic materials is decreased, the coercivity (Hc) increases until the diameter reaches a critical value r_c (a few tens of nanometres), as shown in (Fig.2). At this value the particles start to convert from a multi domain regime to a single domain regime. Each material has a certain r_C value that depends on shape, temperature and crystalline magneto-anisotropy of particles [4].

In small nanoparticles, the increase of coercivity in the single region is due to the level of anisotropy and to the capability of the reversal of arrangement of magnetisation of particles [5]. When the value $r_c \leq r_0$ (~ 10 nm), the coercivity falls to zero due to the effect of thermal energy which leads to randomisation of the moments of the particles at this region [1]. This region is described as superparamagnetic, and the thermal energy in this region is sufficient to change the direction of magnetisation of the entire crystallite. Thus the material behaves in a manner similar to a paramagnet [5].

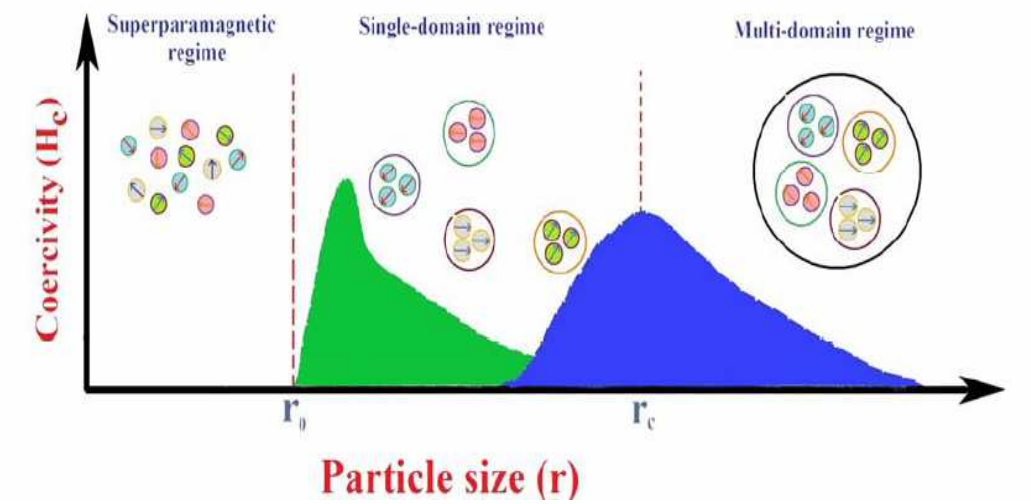

Figure 2: Schematic shows the relationship between the coercivity with particle size. It shows three regions: superparamagnetic, single-domain and multi –domain [5].

Blocking temperature (T_B) is an important feature of the superparamagnetic behaviour [5]. Above this temperature, nanoparticles can behave as a superparamagnetic material, as the temperature increases, the size of particles decreases [1]. Some antiferromagnetic oxide nanoparticles such as CoO and NiO demonstrate weak ferromagnetism at low temperatures [1]. Fig. 3 (a) and (b) shows the zero-field cooling (ZFC) and field cooling (FC) magnetisation versus temperature curves for 3 and 7 nm NiO nanoparticles respectively. The T_B of NiO nanoparticles with size 3 nm is smaller than that of the 7 nm that means such a proportionality between T_B and practical size is noticed.

In addition, the surface and interface effects become more efficient when the size of the particles decreases, where high percentage of the atoms is surface spin. For example, 60% of the total number of spins of fcc cobalt with size nearly 1.6 nm are surface spins [5]. The large ratio of the spin atoms enhance the magnetization and break the symmetry in the particles which lead to band structure changes, lattice constant and/ or atom coordination [5]. As sequence, surface anisotropy or core-surface exchange anisotropy can occur [5]. Peck and his colleagues [10] synthesised Ni (core)/ NiO (shell) nanoparticles with 8-12 nm and shell thickness 2-3 nm. The value of magnetocrystalline anisotropy became close to that of bulk Ni and depends on the size of the Ni (core) and the thickness of the NiO (shell).

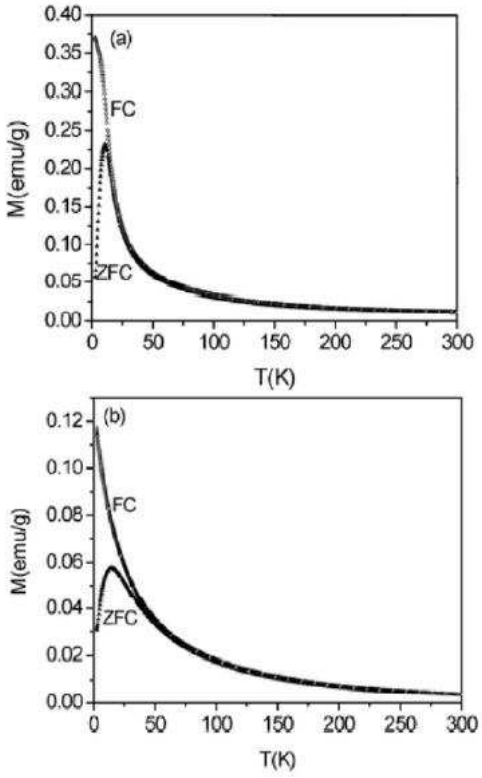

Figure 3: The temperature dependence of magnetization of (a) 3nm and (b) 7nm NiO nanoparticles under ZFC and FC condition (H= 100 Oe) [1].

1.1 Application of magntic nanoparticles

Ni nanoparticles and the (Ni) core/shell system have useful applications in different scientific fields. They can used as active catalysts [11] and there are also various biomedical applications including target cancer diagnosis ,chemotherapy [1, 10, 12-14], drug delivery [12], hypothermia and bioseparation [15].

Guo et al (2009) observed that attached Ni nanoparticles with anti-cancer drug daunorubicin[12] or with positively charged tetraheptylammonium [13] work effectively on (SMMC-7721) liver [13] and leukemia [12, 14] cancer cells. Ni nanoparticles have improved the permeability of cancer cell membranes [12, 13] and have been proven to prevent proliferation of cancer cells [13].

Micronised Ni-Cu alloy has been used in hyperthermia therapy to treat cancerous tumours[16]. The treatment depends on producing magnetic nanoparticles with the desired Curie temperature. Ni-Cu with weight ratio 71% - 29% showed temperatures between 43-44° [16]. Yan et al [11] were successful in developing an easy, active and economical method to protect Ni nanoparticles from environments conducive to oxidation (air and water). They used a starch to protect the surface of synthesised Ni nanoparticles. It was observed that the synthesised Ni particles with starch remained active for 6 more days than those which were uncoated.

Ni/NiO nanoparticles were used for separating and purifying His-tagged proteins from a multi-component solution including a cell lysate [15].

2 SYNTHESIS METHOD

2.1 Synthesis of magnetic metal nanoparticles

Ni nanoparticles were synthesised with a number of different compositions and phases using efficient methods in order to achieve shape-controlled, highly stable and narrow size distribution. Recently, several popular methods including coprecipitation, microemulsion, thermal decomposition, solvothermal synthesis and sol gel synthesis have been employed in the production of Ni nanoparticles [1, 4,5].

This chapter includes the most significant physical and chemical methods used in the synthesis of Ni nanoparticles.

2.1.1 Chemical methods

2.1.1.1 Thermal decomposition

Thermal Decomposition is a well-known method to synthesise high quality monodisperse magnetic nanoparticles with control over size.

This method depends on high temperature thermal decomposition of organometallic complexes such as $[M(acac)_n]$, (M = Fe, Mn, Co, Ni, Cr; n = 2 or 3, acac = acetylacetonate), in the presence of surfactants such as fatty acids and oleic acid in an organic solvent with a high boiling point [1, 16] . Hou et al [17] have performed synthesis of monodisperse Nickel nanoparticles in the range 3 to 11 nm using Ni $(acac)_2$ in the medium of hexadecylamine (HDA) and trioctylphosphine oxide (TOPO).

Bradley et al [18] prepared nickel particles via decomposition of $Ni(COD)_2$ (COD=cycloocta-1,5-diene) in the presence of polyvinylpyrrolidone and CO reagent in dichloromethane. The synthesis formed (20-30 Å) stable colloidal suspensions of nickel.

Magnetic Ni nanoparticles by reduction with H_2 was studied by Chaudret et al [19]. In using H_2, the resulting materials appeared as agglomerates which are composed of individual Nickel nanoparticles with diameters of 3-4 nm. Luo et al [20] synthesised uniform-sized Ni nanoparticles with different crystalline phases (hcp or fcc) and extremely narrow sized distribution using nickel acetate tetrahydrate as a precursor and octadecene and oleylamine as a solvent. Also, the results of magnetic characterisation showed that the magnetic properties of the hcp nickel nanoparticles are quite different from those of the fcc structure.

It was found that if the metal in precursors is zero-valent, such as in carbonyls, thermal decomposition forms oxide free, metallic nanoparticles [4, 5]. However, it can yield high quality monodispersed metal oxides if the first step is followed by oxidation the nanoparticles either with ambient air or elevated temperature [4, 5]. Recently, Davar et al [21] have synthesised Ni and NiO nanoparticles in a range size (14–22nm) by using [Ni $(aceto)_2$] (aceto = 2-hydroxyacetophenato) as a precursor and oleylamine was as a solvent and a stabilising reagent. The most essential parameters affecting the size and morphology of magnetic nanoparticles are the concentration of reagents, such as organometallic compounds, surfactants and solvents, while crucial parameters for the precise control of size and morphology are the reaction temperature, reaction time, and ageing period [4]. A schematic in Figure 4, shows the function of size, morphology and magnetic properties of nanoparticles with reaction temperature and reaction time [4].

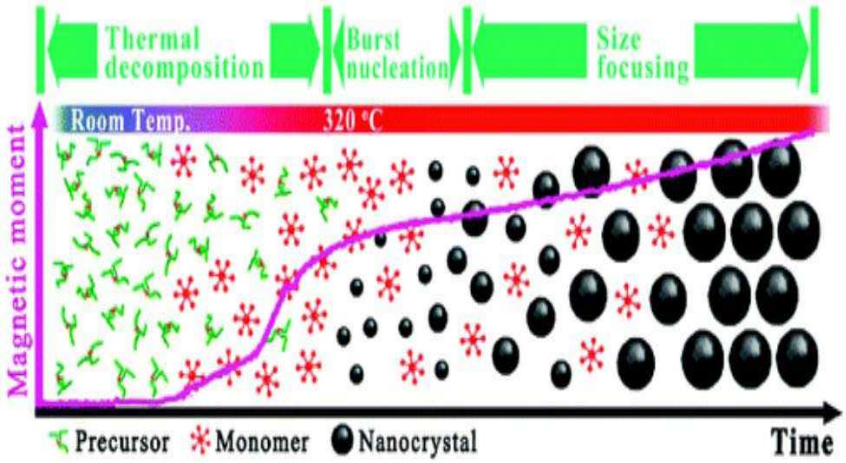

Figure 4: The study of the effect of some parameters on reaction, temperatures and reaction times on the size, morphology and magnetic properties of nanoparticles [5].

Problems relating to the thermal method include high temperatures, complex products, treating the surface of prepared nanoparticles and formation of organic soluble nanoparticles which all serve to decrease their usage in biological fields [4].

2.1.1.2 Reduction methods

Reduction methods are the easiest, oldest and most common methods for obtaining metal nanoparticles. Such methods depend on reducing the metal salts by employing reducing agents in the presence of surfactant materials to synthesise magnetic nanoparticles. The metal salts such as oxides and nitrates in this method are more stable than the organometallic ones which are used in the decomposition methods mentioned earlier [22]. A wide variety of reduction agents are used in this method. However, the most common ones are hydride-based reduction agents such as sodium borohydride and lithium superhydride [22]. Many magnetic nanoparticles are prepared using borohydride as the agent. The borohydride is hydrolysed and hydrogen is released as explained in the following equation [1]:

$$BH^{-4} + 2H_2O \rightarrow BO^{-2} + 4H_2$$

Ni nanoparticles were synthesised by Green and O'Brien [23] using Li or Na borohydride as reduction agent at high temperatures in a basic medium. The disadvantage of this method is that the reaction is incomplete, particularly in the aqueous medium, so the boron appears with products [1]. Hou and Gao [24] used sodium tetrahydridoborate and hexadecylamine (HDA) as stabiliser and solvent respectively to obtain monodisperse nickel nanoparticles of around 3.7nm. By using sodium hydride in organic solvents, dispersed Ni powders were synthesised in the range of less than 4nm[25].

Alcoholic methods which reduce metal salts in the presence of metal particles as the catalyst agent are commonly used in the synthesis of magnetic nanoparticles. The mechanism of the reduction suggests the formation of intermediate complexes, alkoxide and oxonium, which decompose to carbonyl [1]. Teranishi and Miyake [26] prepared uniform Pd/Ni nanoparticles of varying composition by changing the ratio of Ni $(ac)_2/H_2PdCl_4$ (the initial materials) and used a PVP as a capping agent in a propanol medium.

However, by using polyols as reduction and stabilisation agents, large magnetic nanoparticles can be formed [1]. The rate of the reaction can be controlled by monitoring the reaction steps. Hinotsu et al [27] noticed the effect of hydroxyl ions and they used solvent on the properties of Ni nanoparticles. By increasing the ratio of OH^- ions and using trimethylene glycol (TMEG) instead of ethylene glycol (EG), the morphology of Ni particles changed from micron sized irregular plate-like structures to spherical particles with an average diameter of about (16-50 nm). Also, the magnetic properties decreased as a result of the formation of the hpc as well as fcc structure, which is due to the magnetic strength of the hpc structure being weaker than the fcc. Recently, organic alcohols with long chains (hexanol and benzyl) were used as reduction solvents to prepare Ni nanoparticles by Mollamahale et al [28]. Hexanol was effective in controlling the size of these particles.

Other reducing agents

Another method depends on reduction metal halides by alkali metals such as K, Li, and Na in dry THF, diglyme or other ethers to synthesise metal nanoparticles [8]. $NiCl_2$ was reduced to Ni in diglyme by Rieke el al [1] by synthesizing Ni nanoparticles were in THF medium using lithium metal and arene[29] or 4,40-di-tert-butylbiphenyl (DTBB) [30] as catalysts under mild conditions.

A pure Ni nanoparticle with fcc structure and different magnetic properties was prepared using hydrate hydrazine as a reducing agent in the presence of different capping materials [31-33].

2.1.1.3 Sol gel

This in an important method for the production of high purity metallic magnetic nanoparticles with controlled composition. It is a versatile, low-cost and low temperature method, based on the hydrolysis and polycondensation of a sol to form a gel.

Sol-gel synthesis is used to obtain materials with different shapes, such as porous structures, thin fibres, dense powders and thin films (Fig.5). The gel can be formed in different shapes such as a xerogel by evaporating the sol and may be formed as aerogel by drying the sol under supercritical conditions[34] .

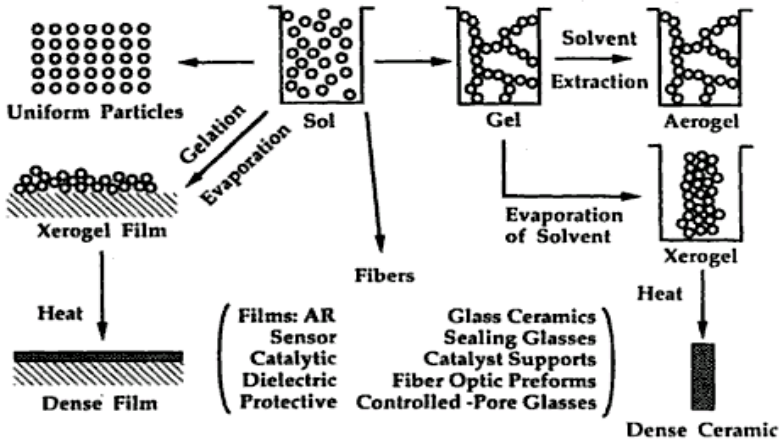

Figure 5: The process of sol gel [35].

This method is valuable for synthesising homogenous nanoparticles of controlled size and shape, at low temperatures [34].

High high-quality Ni nanoparticles and their alloy powders of controlled structure, morphology, size and size distribution were synthesised by this method. It was found that the phase structure and the magnetic properties for the Ni Nanoparticles were affected by applied temperature [34, 36].

2.1.2 Physical methods

2.1.2.1 Arc discharge

Arc discharge is a well developed, high control and powerful method with the high stability of an electric arc system. It is used to synthesise pure metallic nanoparticles by utilising the energy of the arc to melt and evaporate metals in an inert atmosphere. This system depends on thermionic emission of electrons from metals electrodes after beating an arc. Arc discharge has been used in a variety of devices such as arc lamps, welding machines, gas heaters, chemical reactors, arc furnaces and plasma spray equipment. Wei et al [37] used plasma to make a uniform microstructural Ni nanoparticle. The characterisation of these particles was a specific surface area (14.23m2/g) accompanied by narrow particle size distribution (20-70nm). Weber et al studied the catalytic properties of synthesised Ni nanoparticles [1]. Recently, Chang and Su [38] used arc-submerged nanofluid technology to synthesise superparamagnetic Ni nanoparticles under vacuum conditions.

2.1.2.2 Supercritical fluid

A supercritical fluid is an alternative organic solvent in the industrial environment. Its properties lie between those of a gas and those of a liquid. Carbon dioxide and water are the most common supercritical fluids and are used in different fields. Flow-through supercritical water (FT-SCW) method has been used extensively to produce size-controlled free metal

oxide nanoparticles [39]. It is easy to control the reduction reactions by producing a homogenous system. Sue el al [40] prepared Ni and NiO nanoparticles in basic solution at high temperatures. It was noted that with increasing reaction time and magnetisation saturation there was a corresponding increase in the size of particles.

2.1.2.3 Spray pyrolysis

Spray pyrolysis is a powerful technique used to achieve a wide variety of high purity, control composition morphology and produce large quantities of metal, metal oxide, non-oxide and composite powders with uniform size distribution and high crystallinity [33].

Simply, nanoparticles are deposited by spraying small droplets of a solution from a nebulizer onto the heated area of a furnace. Particles of different size can be obtain by controlling the energy of the nebuliser, vapour pressures of the gases and the furnace temperature [1]. The first Ni nanoparticles were synthesised by Nagashima by using H_2–N_2 system over several seconds[33]. Good quality crystallinity and oxidation resistant dense spherical Ni particles were made below melting point by the ultrasonic spray pyrolysis method [40].

Some studies have been carried out using other reducing agents such as NH_3, C_2H_5OH and a set of cosolvents [33]. Wang et al [33] made Nickel nanoparticles by using hydrogen, formic acid, and ethanol set to reduce nickel nitrate hexahydrate at low pressure and high temperature. Low pressure spray pyrolysis technology produces dry nanoparticles with controlled size and morphology on a large scale.

2.1.2.4 Microemulsion method

Microemulsion technology is an straightforward method widely used for controlling the size and morphology of nanoparticles. To date, it has been applied to synthesise spherical and monodispersed nanoparticles by dispersion of a continuous oil phase in nanosized droplets of water[41]. The surfactant and co-surfactant molecules are used to stabilise phases at the

water/oil interface. It is common to synthesise nanoparticles due to their microenvironment. This method has been used extensively to produce a wide range of metallic nanoparticles materials such as metal sulfides, selenides, borides and organic polymers. The disadvantages of this method are adsorption of surfactants on the surfaces of particles which increases the aggregation of particles and the difficulties of forming some metal nanoparticles [41]. Chen and Wu [42] used a water/CTAB/*n*-hexanol set to obtain nickel nanoparticles. Increasing the ratio of CTAB to *n*-hexanol was found to be a critical factor in determining the size of particles, while the high ratio of surfactant to water and the nickel ion were suitable conditions to fabricate small, well-dispersed nickel nanoparticles in PVP/ethanol/toluene/water [41].

2.2 Protection/stabilisation of magnetic nanoparticles

Magnetic nanoparticles have certain properties, such as a large specific surface area, a magnetic dipole interaction as well as the ability to readily react with other materials. These properties make them unstable over long periods of time against agglomeration, precipitation or oxidation under ambient conditions. Forming oxide layers on the surface of particles especially metals and their alloys, lead to changes in the way they behave. Therefore, it is necessary to protect magnetic nanoparticles and their properties by developing efficient procedures to prevent the oxygen from reaching the surface of magnetic nanoparticles and forming larger clusters.

This paragraph concentrates on the procedures for protection of magnetic nanoparticles against oxidation and erosion by acid or base. The core–shell has been successfully applied to isolate the core from the environment. There are two strategies for coating the core: either by organic shells (surfactant and polymersor), or with inorganic shells (silica, carbon, metals or oxides).

Surfactants or polymers are commonly used for preventing the agglomeration and stabilisation of nanoparticles by creating repulsion forces which achieve the balance between the magnetic and van der Waals forces. Magnetic nanoparticles can be coated with an organic shell either during or after the synthesis. When this method employed in situ, the size of nanoparticles will be limited [4]. Both natural and synthetic polymers are used to obtain nanoparticles. The most common natural ones are dextran, and gelatine, while the synthetic ones are polyethylene glycol (PEG), polyvinyl alcohol (PVA) and poly (*N*-vinyl-2-pyrrolidone) (PVP). The main disadvantage of applied polymer coating is that the magnetic nanoparticles can become inactive in reaction with other materials and this layer can be easily removed in acidic medium. As the magnetic properties of these nanoparticles will be affected, most of the research used additional protective layers [4].

Coating the metal core with metal can change the dielectric constant of the region surrounding the system (core/shell) in comparison with the organic shell [1]. In addition, this method can be used to obtain trilayered particles (Pd–Ni)–Pd [1].

Pd Alloys with 3d transition metal (core/shell) has a giant magnetic moment [26] and high catalytic activity [43, 44] and hence synthesis of Pd/Ni particles has been pursued. Pd/Ni was synthesised by different methods in the presence of PVP [43, 44].

Pd-coated Ni (0.5-1%) was previously reported to have a more efficient catalyst in comparison with colloidal palladium, platinum catalysts and commercial (5 wt %) Pd/C [43]. The resistance of particles towards the acid is increased by coating the Ni/SiO_2 with carbon [45].

Coating the nanoparticles with oxide can influence the properties of these particles and increase their applicability. For example, using silica as a dielectric layer increases the resistance of the core towards oxidation, aggolmerisation, photodegradation and acid medium

[5, 46]. In addition, it is easy to modify the surface and the structure of particles and control the interactions between them within the solution and structure by changing the thickness of shell [5]. Most methods of coating with silica depend on hydrolysis of tetraethylorthosilicate (TEOS) in a basic medium [5, 46-48]. The mechanism of coating nanoparticles with silica is shown in Fig.6. The effects of changing the concentration of basic agent (ammonium), water and tetraethoxysilane (TEOS) and other reaction parameters such as aging time on the iron and its oxide nanoparticles were investigated [5, 46, 47]. It was noted that the thickness of shell can be tuned by varying the concentration of ammonium and the ratio of tetraethoxysilane (TEOS) to H_2O [46]. In addition, adding a primer agent such as gelatine facilitates the attachment of silica with particles. This is due to functional groups in gelatine such as –NH2, C=O, -COOH and conjugate acids or bases. The bonding of gelatine with metal particles depended on the pH of the reaction medium [49]. Wang and Harrison method [47] depends on coating the synthesised Iron nanoparticles with silica, both with and without the presence of gelatin. In this work this method was applied on the synthesised Nickel nanoparticles. The reaction of this process can be described as this equation [46]:

$$\text{Ni nanoparticles} + Si(OC_2H_5)_4 + NH_3 + H_2O \longrightarrow \text{Ni nanoparticles-}SiO_2 + 4C_2H_5OH + NH_3$$

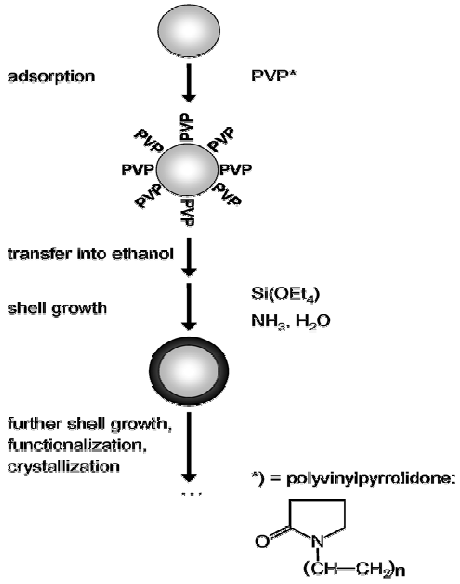

Figure 6: The general mechanism of coating nanoparticles. Firstly PVP is deposited on the surface of

particles. Next it transfers to the medium. Finally tetraethoxysilane Si (OEt_4) is added to medium to form a silica shell around the particles [46].

3 INSTRUMENTATION

3.1 Scanning electron microscopy (SEM)

SEM has widespread applications in many research and technology fields where higher resolution and low beam energy are important. It is used to create three-dimensional images with nanoscale resolution that can be easily interpreted. Also it can monitor the growth of thin films and nanostructures.

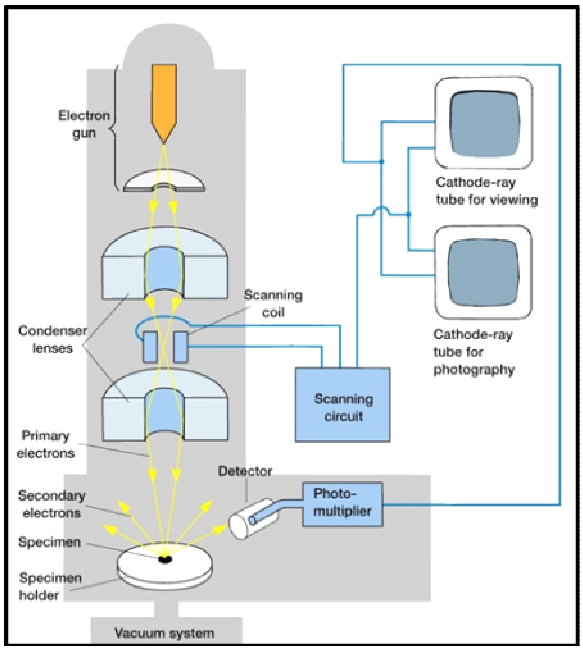

Figure 7: A schematic diagam of an SEM. Instrument.

The basic principle of a scanning electron microscope (SEM) is as follows. The finely focused electron beam is projected across a specimen to produce a signal, and the intensity of signal depends upon the shape, chemical composition and crystal arrangement of nanoparticles. A schematic diagram of an SEM is shown in (Fig.7). The electrons are emitted from a hot tungsten filament, lanthanum (LaB_6) or a field emission (FE) tip. The

electrons are then accelerated towards the sample by applying a high negative voltage (1 to 30 KV). The normal method is to make the FEG/Tungsten tip negative (-1 to -30 KeV) relative to the earthed anode, thus, the electrons "see" a positive potential and are attracted (and accelerate) towards it.

Two or three condenser lenses are used to focus the electron beam into a small spot of about 5 -50nm in diameter. The two lenses closest to the electron gun are called condenser lenses. The lens closest to the sample is called an objective lens, which moves the crossover of the electron beam up and down until it strikes the specimen surface. The scan of the sample occurs when the magnetic field is produced by varying the voltage by the scan generator in the scan coil, which deflects the beam back and forth. When the electron beam, typically with energy of 1-30 KeV, irradiates the specimen, and secondary electrons, backscattered electrons, characteristic x-rays and other types of radiation are emitted from the surface of sample. Primary electrons generate low energy secondary electrons (around 10-50 ev), which demonstrate the topographic features of the specimen. These secondary electrons are collected by an Everhart-Thornley (E-T) detector, accelerated to 12KV and they strike a scintillator producing light. This light is amplified by a photomultiplier tube (PM) to produce an electrical signal.

The signal is displayed on a monitor. The relative signal is strengthened from a "shadow" effect of the sample, which can be interpreted as a "3D" image. The "3D" is derived from the position of the detector relative to the specimen. It is possible to obtain images of a comparatively large area of the sample. The specimen in SEM should be dry and covered with conducting layer, either of thin metal or graphite in order to avoid charging. The microscope is evacuated to a high vacuum to prevent scattering of the electrons. A FEI/Philips XL-30 FEG (Field Emission Gun) SEM instrument (see Fig.8) was employed for the characterisation of the Ni nanoparticles and Ni coated with Silica in this work.

Figure 8: A Philips XL-30 FEG SEM instrument.

3.2 Energy dispersive x-ray spectrometry (EDX)

EDX is a quick method for identifying and quantifying the elements in specimen on a micron scale. This instrument has many applications in different fields and is capable of analysing a wide range of specimens. When the material is irradiated with a high energy electron beam, electrons are ejected from the inner shells of the atoms. This process leaves a vacancy within the electronic structure of the atom, then that vacancy is filled with an electron from an outer shell. An x-ray is emitted as the result of energetic difference between the shells. The x-rays have energies which are characteristic elements and can be used to identify the chemical composition of the specimen, and can also be used for elemental mapping. It is common to attach this instrument to SEMs and TEMs. EDX has limitations, as it cannot distinguish ionic from non-ionic, isotopic species, and elements with atomic numbers less than carbon ($Z<5$). In this work, a Rontec EDX was used for analysing the Ni nanoparticles and Ni coated with SiO_2.

3.3 Transmission electron microscopy (TEM)

TEM is the most important application for creating atomic-resolution real space images and diffraction pattern for nanomaterials. In addition, TEM can directly determine and quantify the chemical and electronic structure of nanomaterials by focusing on single nanoparticles in a sample. These nanoscale applications make TEM one of the most powerful characterisation techniques for nanoscale materials.

The important application of TEM is electron diffraction, which is used to obtain the three-dimensional structure of crystals, lattice parameters, space group and crystal orientation. Electron diffraction also can be distinguished between crystalline and amorphous materials, where the latter appears as a diffused ring pattern. Nowadays, high resolution transmission electron microscopy (HRTEM) is used to create interference images for crystal structure by using transmitted and scattered beams.

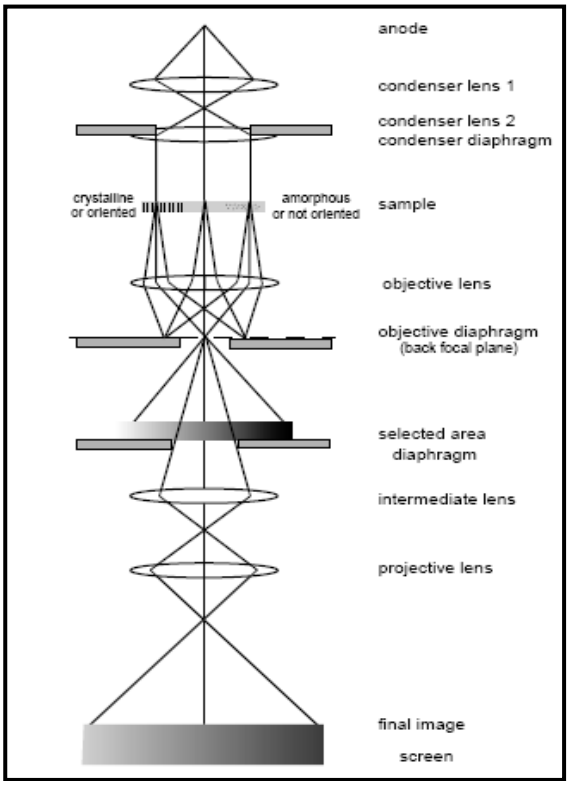

Figure 9: A simplified TEM instrument.

A TEM works in a similar way to the previously mentioned SEM instrument. In TEM, a focused, high energy electron beam (100-400 KV) is transmitted through an ultra-thin sample to provide important information about morphology, crystallography, particle size, and distribution and atomic-resolution lattice images. The dark field (DF) and a bright field (BF) give images in nanoscal. The image is formed when the electron beam strikes a phosphor screen or charge coupled device (CCD) camera, after it passes through a magnifying lens. A simplified TEM instrument is shown in (Fig.9)**.** There are some limitations in TEM, most of which are related to specimen, for example irradiation damage, in particular the biological sample from the electron beam and difficulties in characterising the whole sample due to field of view.

The TEM measurements of Ni nanoparticles and Ni coated with silica, in the work to be reported here were carried out using a CM 30 and CM 200 Philips instrument.

3.4 X-Ray diffraction (XRD)

X-ray diffraction is one of most powerful non-destructive analytical techniques for determining the crystal structure and grain orientation of nanomaterials. The applications of this method include: identifying and quantifying various crystalline phases of powder and solid materials, all of which determine the physical properties of the sample. Crystalline size, microstrain and macro-stress can also be evaluated.

The diffraction pattern is produced by diffraction of the X-rays by different planes of the regular crystalline sample. It is possible to get information about the atomic arrangement within the crystal from X-ray diffraction patterns. The patterns can be identified by comparing them with internationally known databases such as the International Centre for Diffraction Date (ICDD) powder diffraction file. The PDF4+ database contains approximately 135,000 powder diffraction patterns.

The critical factor for achieving good results in X-ray diffraction is the preparation sample. Samples should consist of randomly orientated crystallites and should be flat, smooth and of the correct height. XRD has limitations, in that it cannot be used to study amorphous materials.

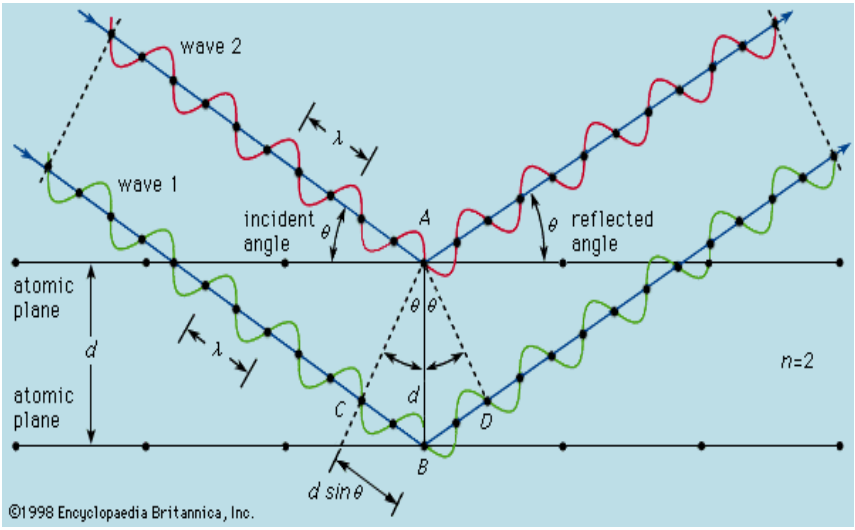

Figure 10: Constructive interference condition.

Diffraction is a constructive interference phenomena (see Fig.10), which occurs when monochromatic X-rays with wavelength λ are scattered by the individual atoms of crystal at a given angle θ of incident beam. These atoms form sets of parallel planes separated by a distance *d*. The constructive interference occurs when Bragg's law is fulfilled:

$$n\lambda = 2d\sin\theta$$

X-ray diffraction is based on Bragg's law. This law involves a sharp diffraction for the crystalline broadening that occurs when the crystallites are small (submicron) and/or the lattice is strained. In 1918, Scherrer observed the relationship between microstructure and the diffraction pattern. He derived a well-known equation describing the relationship between the crystallite size and the peak width, which is called the Scherrer formula: $t = K\lambda/(B\cos\theta)$, where t represents the size of the crystallites, λ is the wavelength of X-rays,

B is the integral breadth or the width of the diffraction line measured at half the maximum intensity. K is the Scherrer constant, which depends on the geometry of the crystal in range from (0.89-1.39); K=0.89 for spherical wave of two dimension lattice, K= 0.94 for cubic three-dimensional crystal, K=1.33 for typically spherical specimen[2]. This equation can be used to evaluate the crystallite size of nanomaterials.

A typical diffraction pattern is produced by plotting the diffracted intensities versus the diffraction angle, 2θ (the angle between the incident and reflected rays). In modern powder diffractometers the intensities of reflections are collected electronically, as the detector is rotated around the sample in a plane of the incident beam.

There are three important parameters in a diffraction pattern: the position of the diffraction lines, the intensities of the diffraction line, and the width of the diffraction line. The positions and intensities of the diffraction lines are used to determine the unit cell dimensions. The

width of the diffraction lines can be used to evaluate the crystallite size or lattice strain.

In this work, X-ray diffraction studies for the characterisation of nickel nanoparticles and nickel coated with silica were performed using CuK_{α} radiation (50 kV, 40mA) on a Philips X'Pert (Fig.11) automated powder diffractometer (APD).

Figure 11: A Philips X'Pert materials diffractometer (APD) instrument.

The scanning conditions used for identification of phases were: scan type continuous, scan mode θ /2θ , step size 0.05 ° 2θ, scan range 5 to 85° 2θ, counting time per step 10 seconds, total analysis time 4 hours and 30 minutes.

3.5 Fourier transform-infrared spectroscopy (FTIR)

FTIR spectroscopy is one of the most reliable and commonly utilised techniques for the identification of the functional groups and organic ligands attached to organic /inorganic nanoparticles. It is an accurate and quick method for identification of molecular components and structures. Many substances can be characterised, identified and quantified in any state: solid, liquid, or gas. FTIR can also be used in the study of kinetics of reactions and can detect impurities in substances.

The principle of FTIR technique is that all molecules absorb IR photons except monatomic and diatomic ones which do not have a dipolar moment resulting from charge differences in the electronic fields of the atoms within the molecule. When IR rays irradiate molecules with a dipolar moment, infrared photons interact with the molecule causing excitation to higher

vibrational states. Each molecule absorbs infrared light at certain frequencies. This property provides unique absorption spectral pattern or fingerprint through the entire infrared light spectrum.

Absorption bands in the range of 4000-1500 cm^{-1} are typically due to functional groups (e.g., -OH, C=O, N-H, CH3, etc.). The region from 1400 - 900 cm^{-1} is known as a fingerprint region. Absorption bands in this region are generally due to intramolecular phenomena and are highly specific to each material. Typical FTIR spectra are produced by plotting the wavelength or wavenumber against absorption intensity or percentage transmittance. This technique solves the limitations caused by slow scanning. FTIR spectroscopy is multiplexing, so all optical frequencies from the source are observed simultaneously, rather than individually, over a scan time. This means that the summed absorption of multi-chromatic light is distributed using the Fourier transforms in order to produce a spectrum. The IR studies in this work were carried out using FT/IR-4100 JAS.CO.

4 EXPERIMENTAL

4.1 Synthesis of Ni-Pd nano-particles

Reduction method was used to synthesise Ni-Pd nano-particles. In a three necked flask, 100 mg of $Ni(ac)_2$ was dissolved in 40 ml warm 1-Propanol then 20 mg PVP was added and the mixture heated. When the solution reached boiling point, 5 mg of $PdCl_2$ dissolved in 20 ml 1-Propanol (by sonication) was injected into the mixture. The mixture was stirred vigorously and refluxed for a further 3-5 hours under air. The solution in the vessel turned to brown a few minutes after the injection of Pd ions. When the contents of the flask were cooled to room temperature a black precipitate was obtained.

4.2 Coating of Ni-Pd nano-particles with SiO_2:

Ni-Pd particles were coated with silica shell following two procedures that Wang and Harrison [49] adopted to coat Ni nanoparticles.

Procedure A (witout gelatine): 3.4 mol dm^{-3} water. 0.45 mol dm^{-3} ammonia, and 50 mg dm^{-3} Ni-Pd particles were dissolved to propan-2-ol at room temperature (the total volume of sol was 50 ml) and stirred until particles dissolved. Then, 0.004 mol dm^{-3}, sample 1 (S_1) and 0.002 mol dm^{-3}, sample 2 (S_2) of TEOS (99.999%) were added rapidly. Finally, the reaction mixtures for both samples were aged for 24 hours.

Procedure B(with gelatine): Ni-Pd particles were treated with 1% aqueous gelatine in two ways: the first one Ni–pd particles were refluxed with (5 ml) of a 1% aqueous solution of gelatin for 2 hrs, and then aged at120^{o}C for 12 hrs, sample 3 (S_3).

In the second procedure, the particles were treated with 2.5 ml of a 1% aqueous solution of gelatine at 80^{o}C until it dried by evaporation and the gum-like solid obtained aged for 12

hours at 120^{o}C, sample 4 (S_4). The particulates obtained were further treated with 0.004 mol dm^3 of TEOS as outlined in procedure A.

4.3 Results and Discussion

4.3.1 Ni nanoparticles

XRD pattern (see Fig. 12) revealeess that the samples obtained at the end of reduction step consist of the following phases: cubic Ni (ICDD, PDF4+2009, no. 00-004-0850), hexagonal Nickel hydroxide (ICDD, PDF4+2009, no.00-022-0444) and cubic Pd (ICDD, PDF4+2009, no.04-001-0111). The peaks are broad due to the reduced size of the particulates [21].

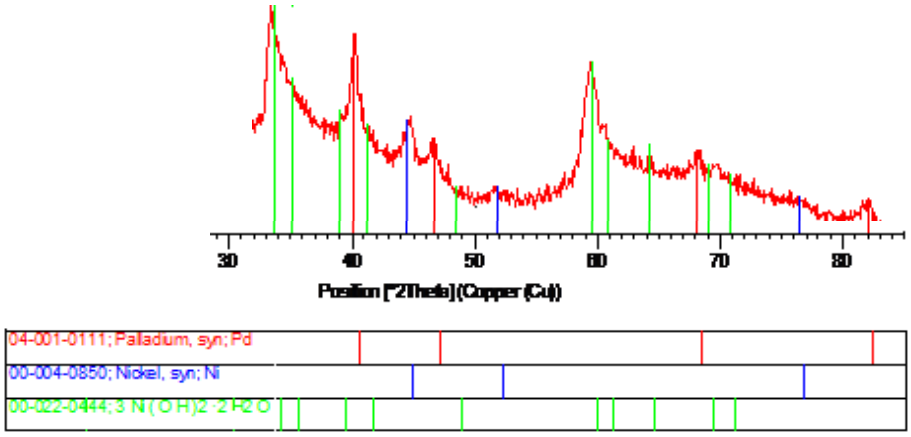

Figure 12: XRD patterns of Ni nanoparticles

In the IR spectrum of Ni nanoparticles (Fig. 13) a new peak is evident at 670.42 cm^{-1} compared with PVP, the capping agent. This peak could be assigned to Ni–O stretching as reported previously [50, 51]. The absorption band near 1613 cm-1 is assigned to H-O-H bending vibrations due to the adsorption of water from air [50].

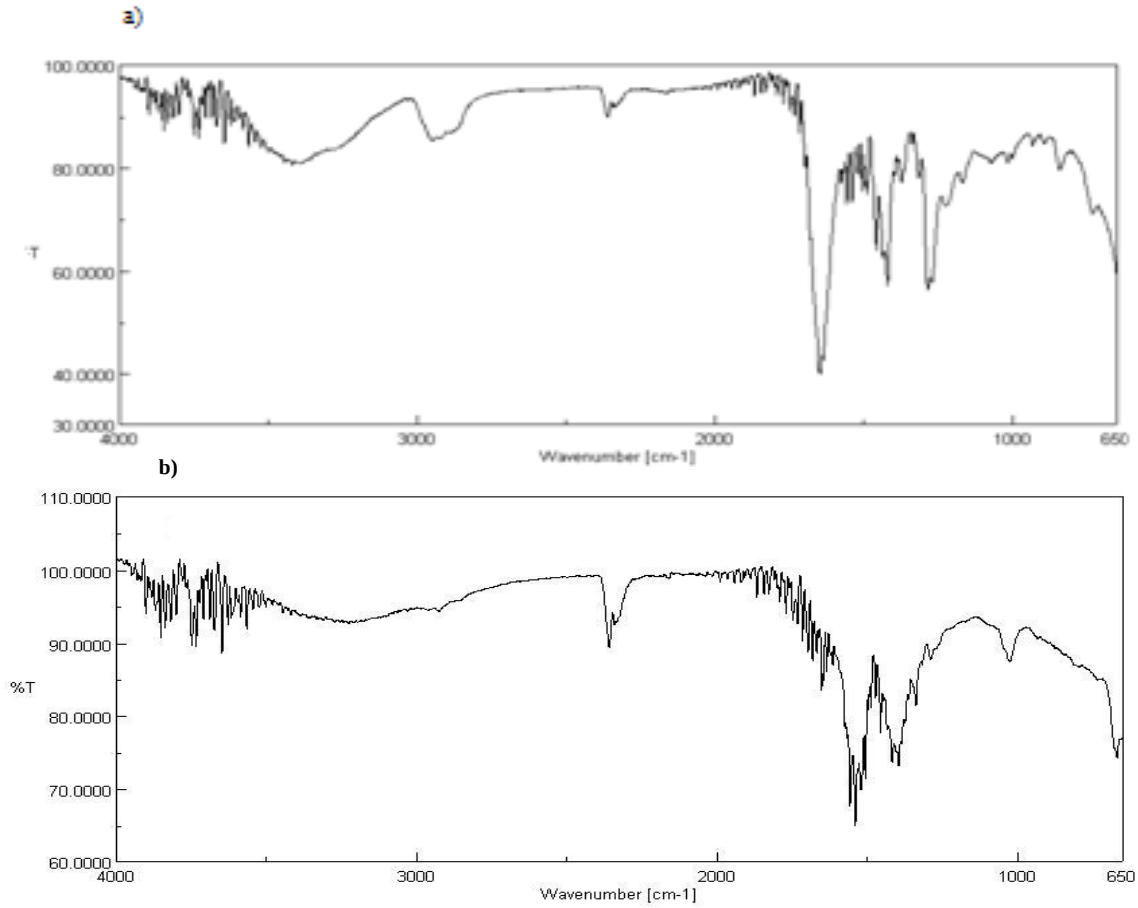

Figure 13: FTIR spectra of a) PVP b) Ni nanoparticles.

EDX spectrum (see Fig. 14) confirms the presence of Pd, Ni, and oxygen. The percentage of oxygen is around 38.8 W%.

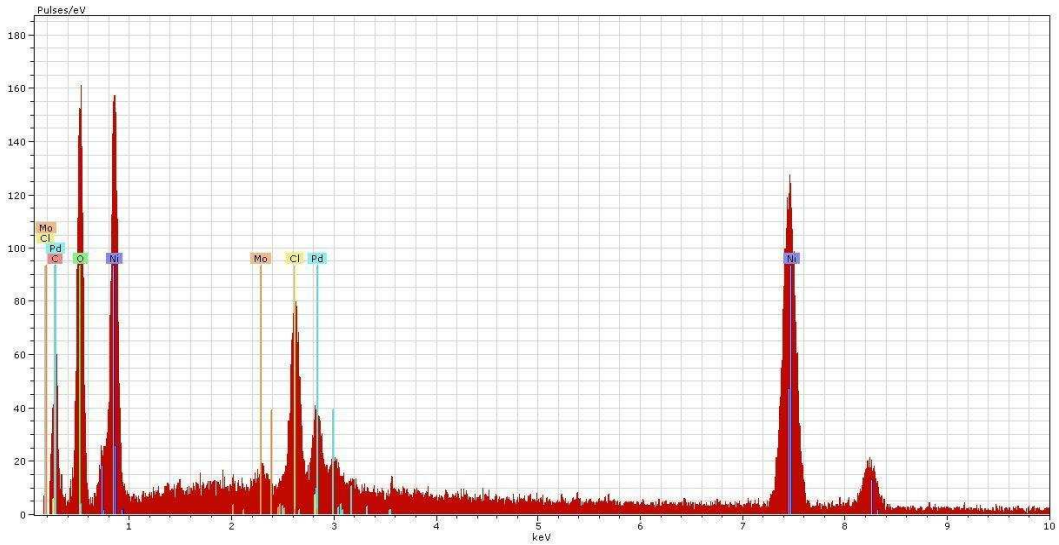

Figure 14: EDX patterns of Ni nanoparticles.

Microanalysis yields hydrogen composition between percentages of ~ 1.5% in all samples. As consequence of XRD, microanlysis, EDX and IR the composite structure of this particles found to have consisting of mixture of Pd, Ni, with the same average diameter and Ni $(OH)_2$ phases, with the NiO phase being amorphous. The precence of Ni $(OH)_2$ and NiO have been noticed in some cases [10, 49,50]. The following diagram shows the likely structure of synthesised nanoparticles (see Fig. 15).

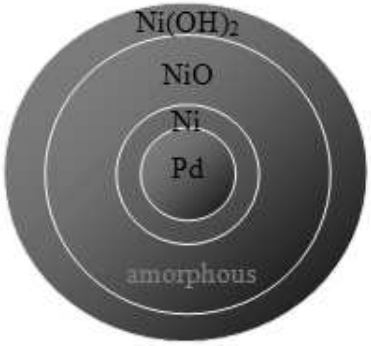

Figure 15: The structure of synthesized Ni nanoparticles.

Spherical Ni nanoparticles with diameters ranging from 2-20 nm were observed in TEM microscopy (see Fig.16). The particles are reasonably monodisperse.

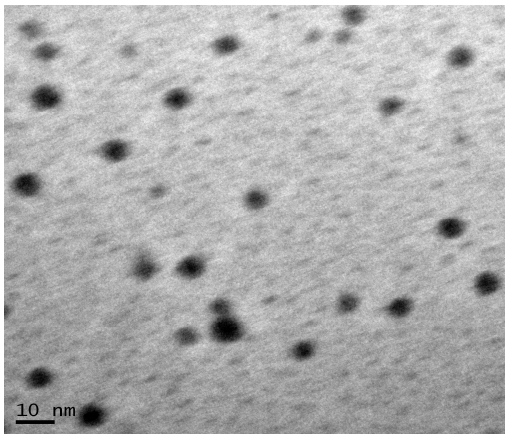

Figure 15: TEM micrograph of synthesized Ni nanoparticles

SEM images of Ni nanoparticles have very angular fine particulates with edge length of several microns consisting of fractured surfaces in low magnification see figure 17 (a, b). we believe that these particles are aggregates of nanoparticles some of which can be seen in high magnification Fig 17 (c, d).

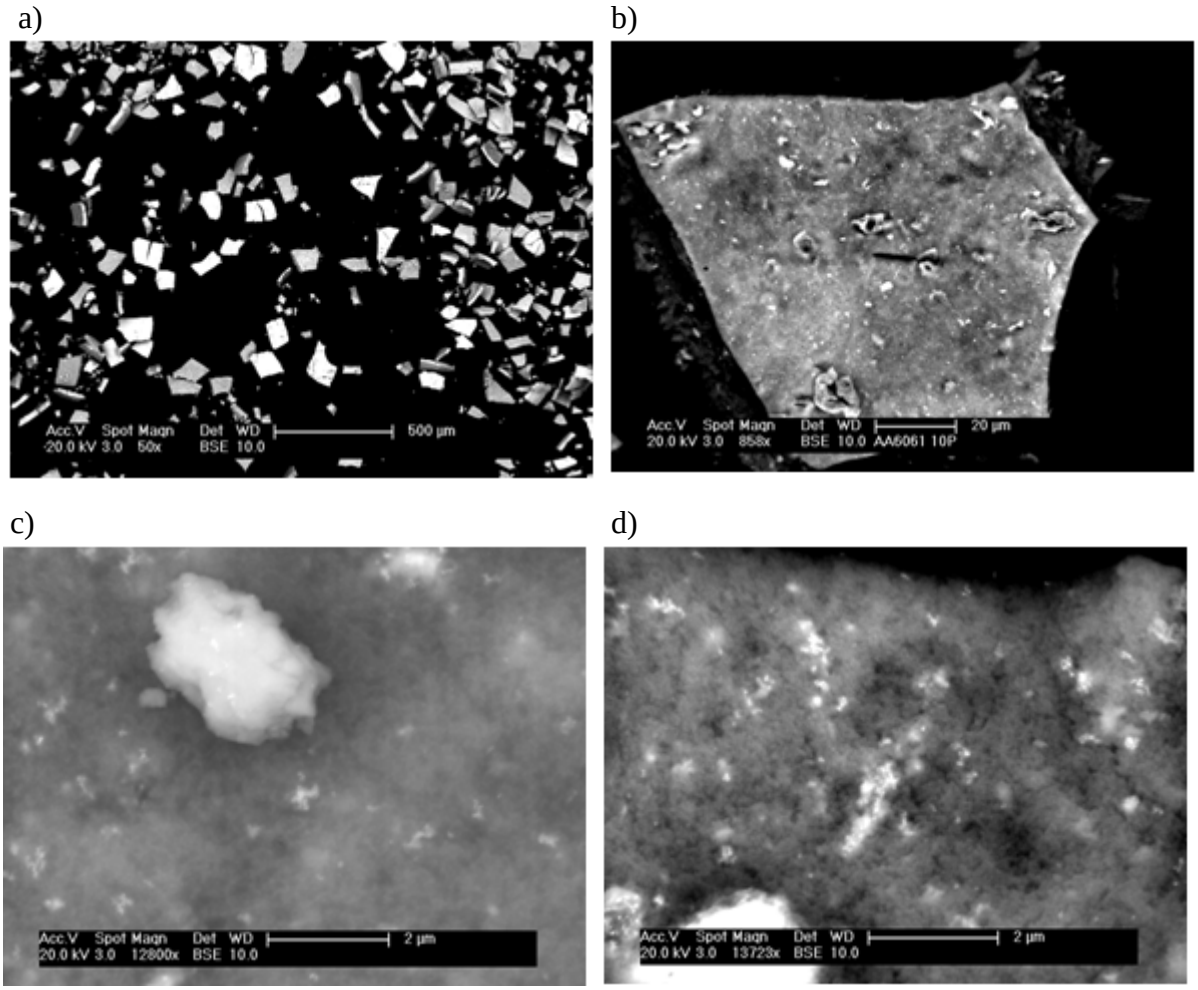

Figure 16 : SEM images of Ni nanoparticles in different magnification.

The magnetic property of Ni nanoparticles has been measured (Fig.18). Zero-field –cooled (ZFC) and field-cooled (FC) magnetization curves were recorded over 5-300 K temperature range with an applied magnetic field of 100 Oe. The particulates are paramagnetic at room temperature and undergo a transition to ferromagnetic phase with a blocking temperature of

about 240 K. The hysteresis loop at 5 K was asymmetric (X1=453 gauss, X2= -531 gauss at Y=0) with respect to zero magnetic field, indicating that there is an exchange biasing effect [10]. It has demonstrated a strong magnetic property (Fig. 18-d), which may be due to the Pd core being surrounded with Ni nanoparticles of the same size [26].

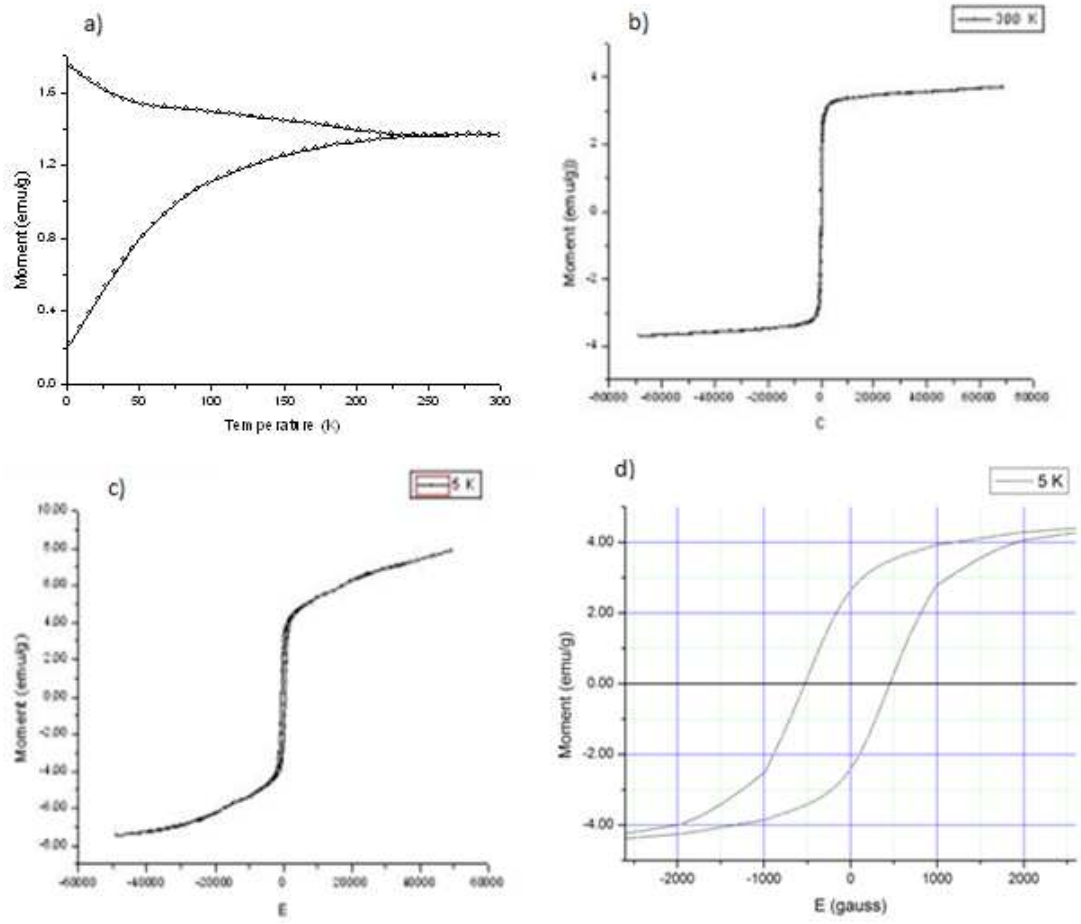

Figure 17: Magnetisation properties of Ni nanoparticles: a) zero-field cooling (ZFC) and (field cooling) FC magnetisation versus temperature b) applied at 300K, c-d) at 5K.

4.3.2 Ni/ SiO_2 nanoprticles

The effects of the concentration of TEOS, ageing time and presence of gelatin on the silica coating are outlined below:

Role of TEOS Concentration and gelatin:

Fig. 19 (a-h) shows the SEM images of both coating Ni nanoparticles with different concentrations of silica, both with and without presence of gelain. In low magnification the upper inset in Fig.19 (b, d, f, h) have shown very irregular particular deposits besides aggregates (a, c, e, g). In high magnification the particles were elongated clusters of spherical/globular particles for S_2 and S_4 (see Fig. 19 - d, h), while Clusters of flattened plate-like particles for S_1 and S_3 as shown in Fig 19 (b, f).

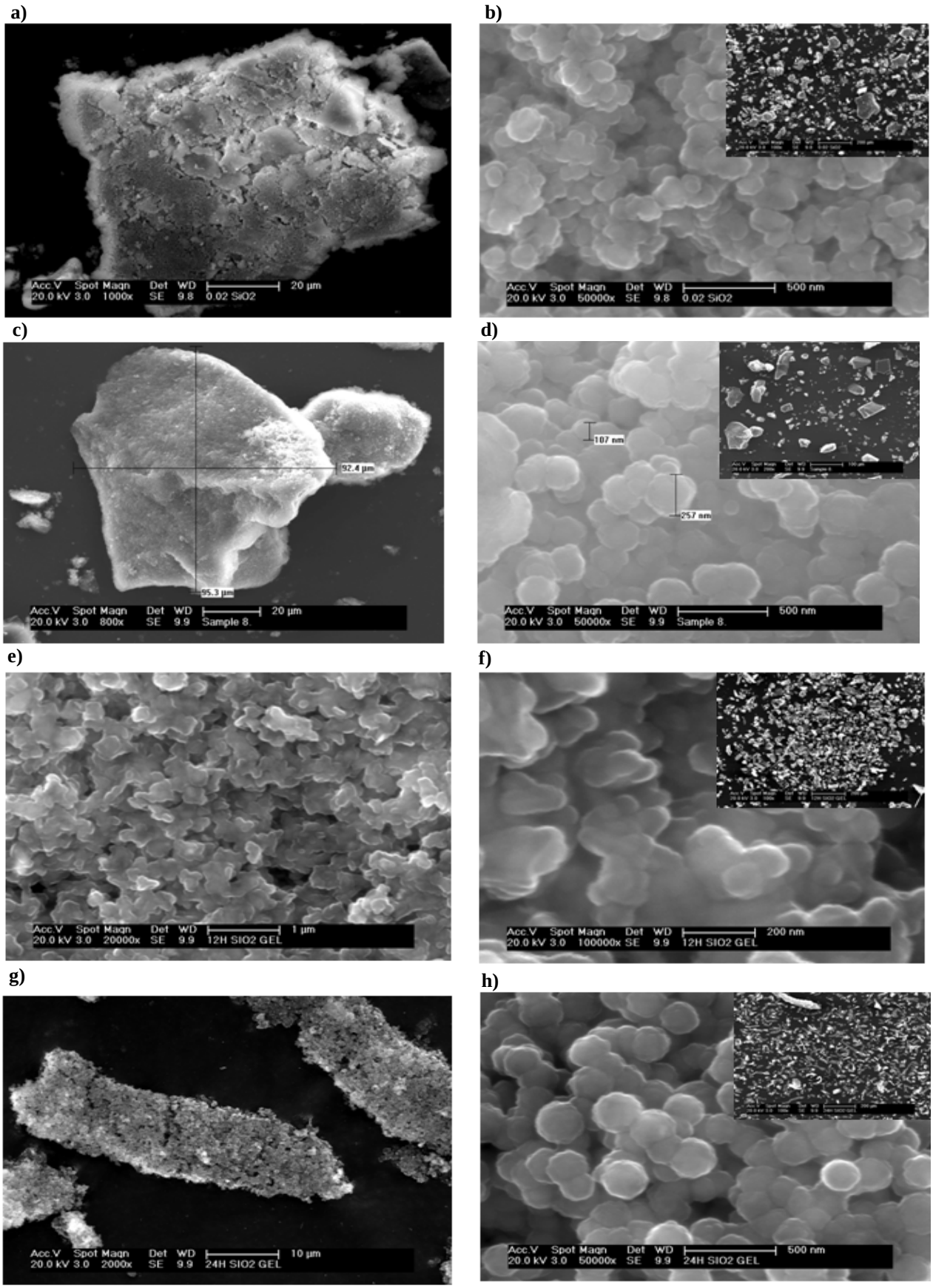

Figure 19: SEM images of a) and b) 0.004 mol dm^{-3} TEOS (99.999%) S_1 c) and d) 0.002 mol dm^{-3} TEOS (99.999%) S_2 e) and f) using gelatine at 100 ° C S_3 g) and h) using gelatin at 80 °C S_4, aged 24 hours, in different magnifications.

TEM images of Ni/SiO_2 nanoparticles (See Fig. 20) have showed that a spherical silica shell with diameter (60-80nm) was successfully prepared using different concentrations (0.004, 0.002 mol dm^{-3}) of tetraethylorthosilicate (TEOS) in an ammonia medium.

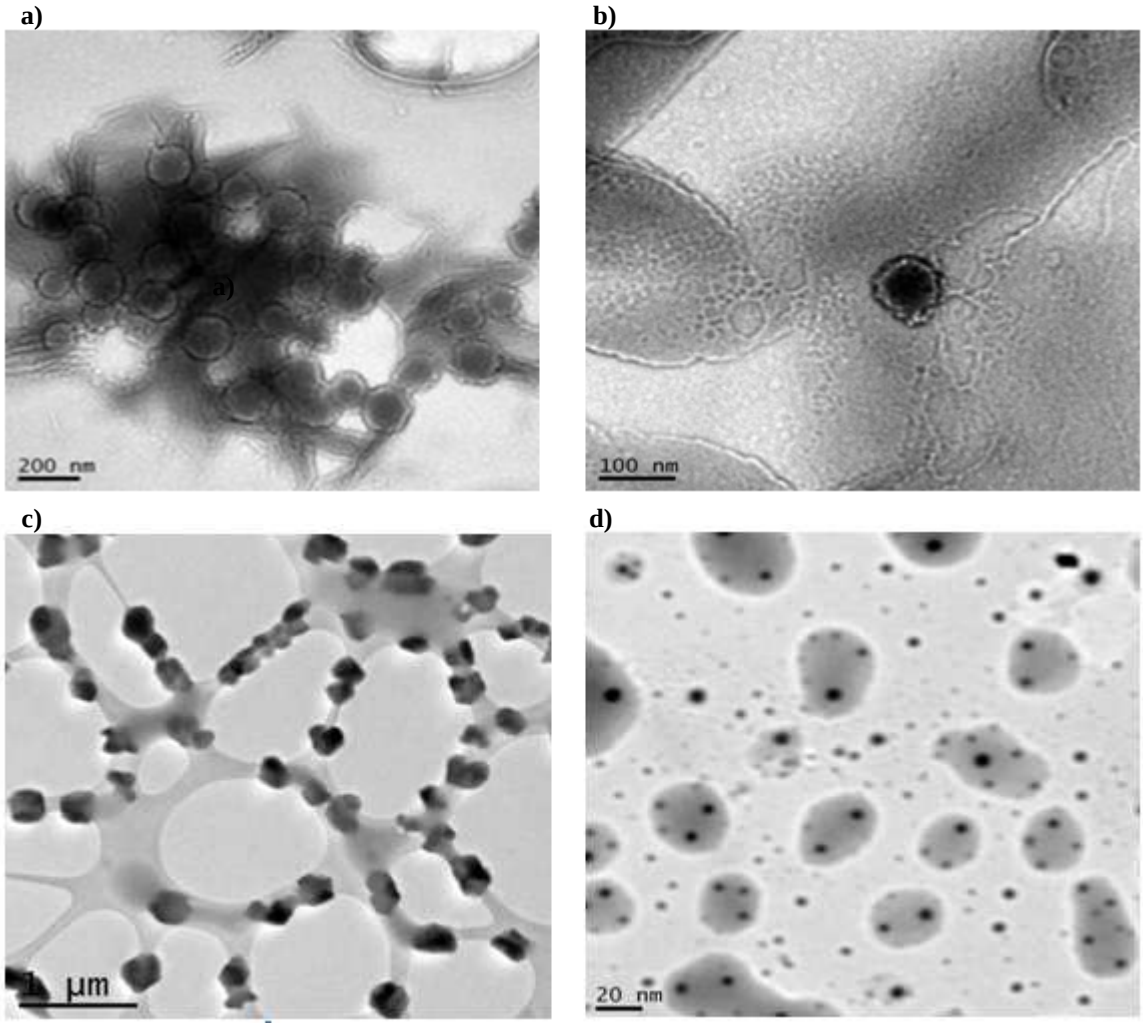

Figure 20: TEM images of a) and b) 0.004 mol dm^{-3} TEOS (99.999%) S_1 c) and d) 0.002 mol dm^{-3} TEOS (99.999%) S_2, aged 24 hours.

Fig. 21 shows the TEM images of Ni nanoparticles in the presence of gelatin as a primer. It was obvious that the presence of gelatin makes the coating process more easy and efficient [47]. In comparison between procedure-1 (without gelatin), see Fig. 20, and procedure-2 (with presence of gelatin), the small particles in the later were coated with silica shell beside the big ones, also the size of shell became smaller 20-44 nm (see Fig. 21)

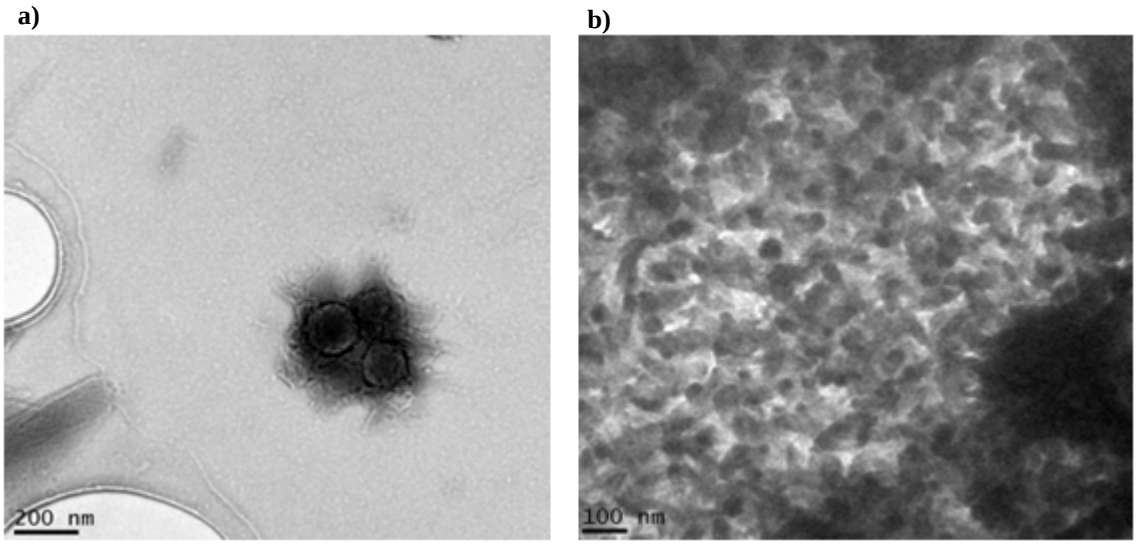

Figure 18: TEM images of a) using gelatine at 100 °C S_3 b) using gelatine at 80 °C S_4, aged 24 hours.

Decreasing the concentration of the TEOS had a significant influence on the shape of silica shells [46]. In comparison between S_1 and S_2, the S_2 with less concentration of TEOS showed less agglomeration of nanoparticles (see Fig. 20 c, d). In addition, TEM and SEM images of S_1 were observed the formation of nanotubes in (see Fig. 22).

The method which used to prepare S_4 (with gelatin and less concentration of TEOS) was more efficient than that used for S_3 (see Fig. 21-a), where the S_4 showed less agglomeration of nanoparticles (see Fig. 21-b). Consequently, the effect of decreasing the concentration of TOSE was studied.

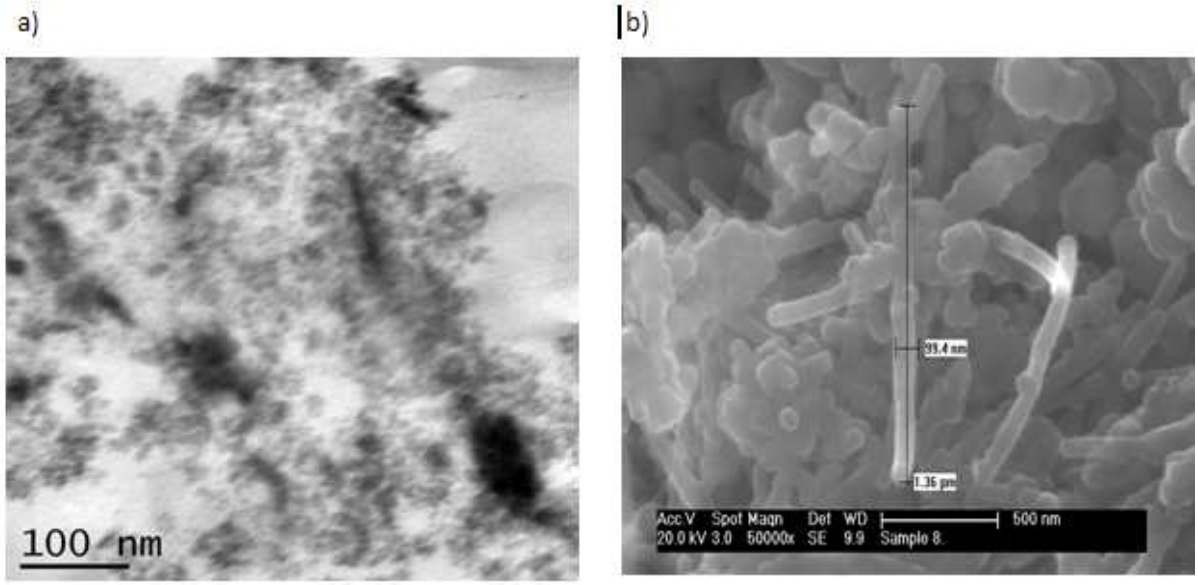

Figure 19: a) TEM images b) SEM images of 0.004 mol dm^{-3} TEOS (99.999%) S_1.

S_2 and S_4 were made in high diluted (10 times in pronanol-1) for studying the effect of decreasing the concentration of TEOS on system (core/shell). The silica shells for both with and without a gelatin became smaller and more spherical, and the precipitate of the silica and agglomeration of the particles decreased (see Fig.24 a-b).

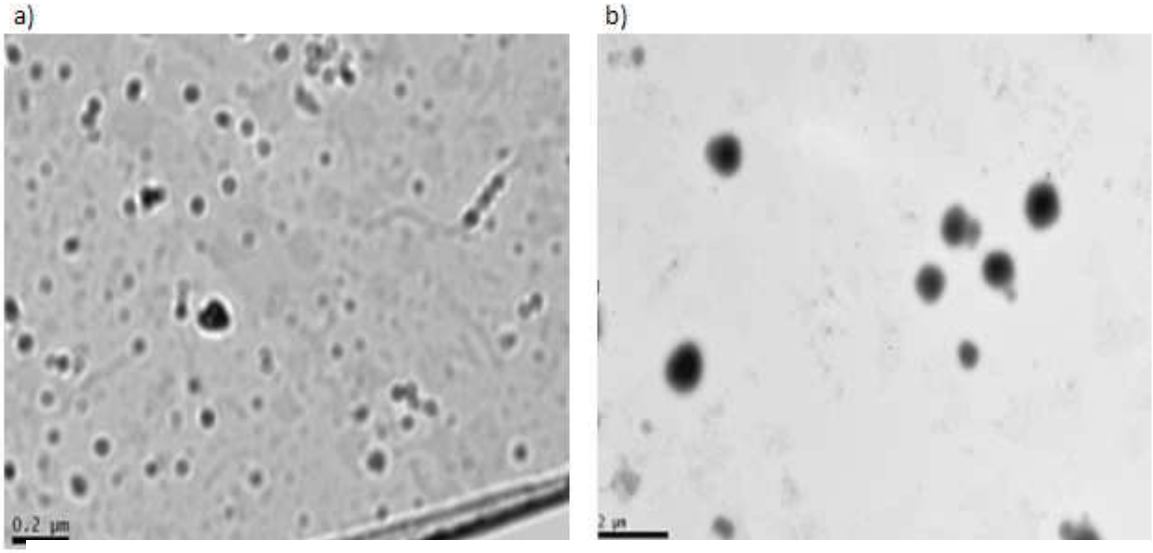

Figure 20: TEM images of high diluted samples a) 0.002 mol dm^{-3} TEOS (99.999%) S_2 b) using gelatin at 80 °C S_4, aged 24hrs.

XRD patterns reveal that the samples obtained at the end of coating with different concentration of silica (S_1 and S_2) and with enhancement of gelatin (S_3 and S_4) consist of the following phases (see Fig.24): cubic Pd (ICDD, PDF4+2009, no.04-001-0111), Nickel hydroxide with a different structure (depending on the concentration of silica and process of coating in the presence of gelatin). Where S_1, S_2 and S_3 have the same phase Rhombohedral $Ni(OH)_2$ 0,75 H_2O (ICDD, PDF4+2009, no. 00-038-0715) as shown in Fig 24 (a, b, c), while S_4 has $Ni(OH)_2$ Hexagonal structure (ICDD, PDF4+2009, no. 00-057-0907) as shown in Fig. 24-d. The XRD pattern of the S_1 was amorphous this is related to high concentration of silica in the sample. It was noticed that the peaks in all XRD patterns are broad due to the reduced size of the particulates [21].

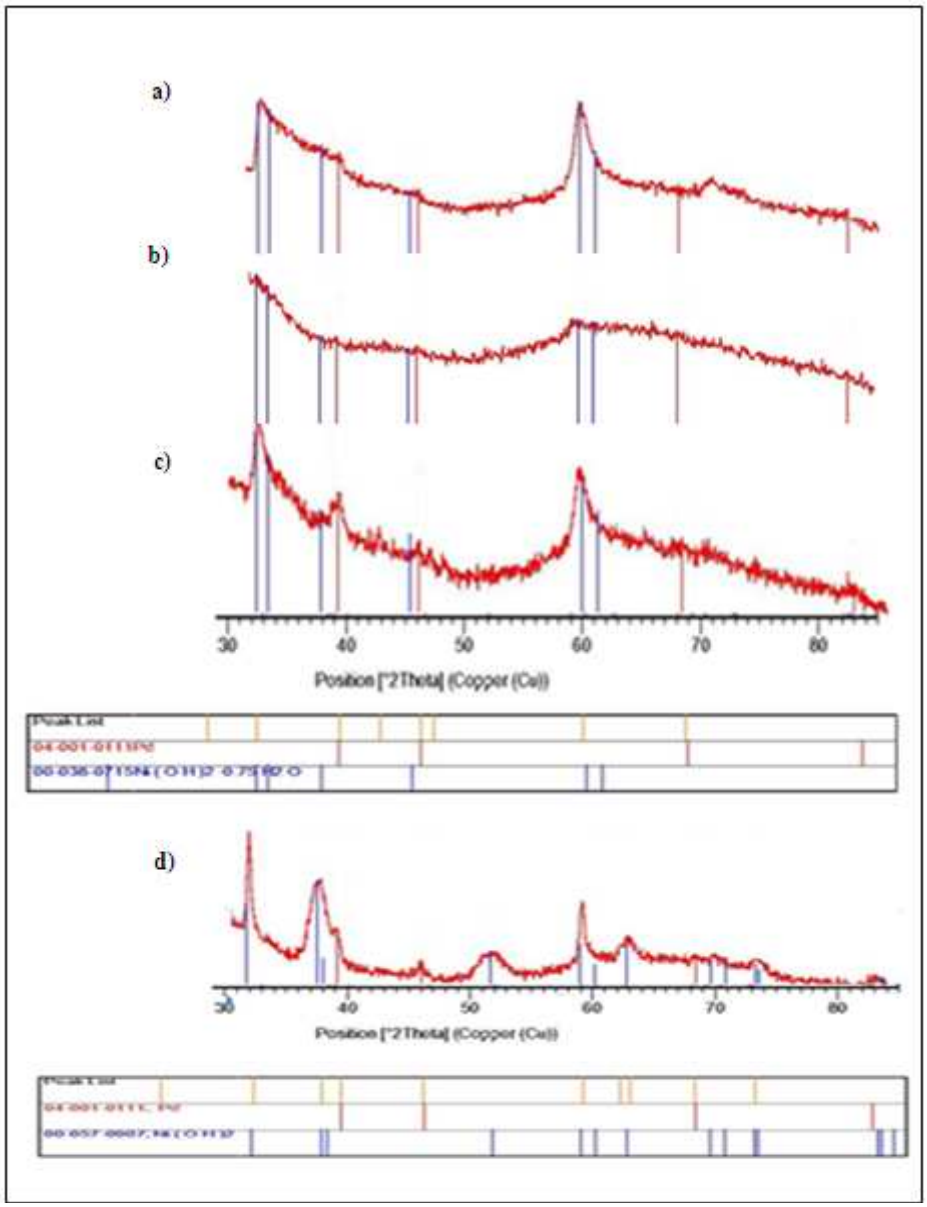

Figure 24: XRD patterns of a) 0.002 mol dm^{-3} TEOS (99.999%) S_2 b) 0.004 mol dm^{-3} TEOS (99.999%) S_1 c) using gelatine at 80 °C S_3 d) using gelatine at 100 °C S_4, aged 24 hrs.

IR spectra of coating particles (Fig. 25 b-f) showed the present of strong band at 1045-1079 cm^{-1}, 795-895 cm^{-1} respectively, corresponding to Si-O-Si stretching bending frequency. Decreasing the concentration of TEOS (see Fig.25) was accompanied by a shift of the Si-O-Si stretching band to lower frequencies and a shift of the Si-O-Si bending band towards higher frequencies. Therefore, IR studies corroborate TEM studies and indicate that the shell formation has taken place on Ni nanoparticles.

The presence of certain peaks at 2900-2960 cm^{-1} (C–H) (see Fig.23 b-f , Fig.17 b), stretching of PVP (see Fig.23-a) carbon chain, absorption peaks at 1640-1697cm^{-1}, C=O stretching vibration on pyrrolidone heterocyclic of PVP [52, 53], peaks at 3100-3500 cm^{-1} (N-H stretching),1550-1640 cm^{-1} (N-H) bending suggests PVP ligands remain coating the synthesised nanoparticles and bound to the surface of nanoparticles by carbonyl group [54-56] or amide groups of PVP [57].

Decreasing the absorption of carbonyl and amide groups suggests that a part of PVP remains in the solution, which corroborates with the EDX (see 22, a-d) studies (absent of nitrogen peaks). It can be seen that there is a presence of NiO and Ni $(OH)_2$ from IR, if the spectrum start from 400 cm^{-1} (there is a limited in the used instrument).

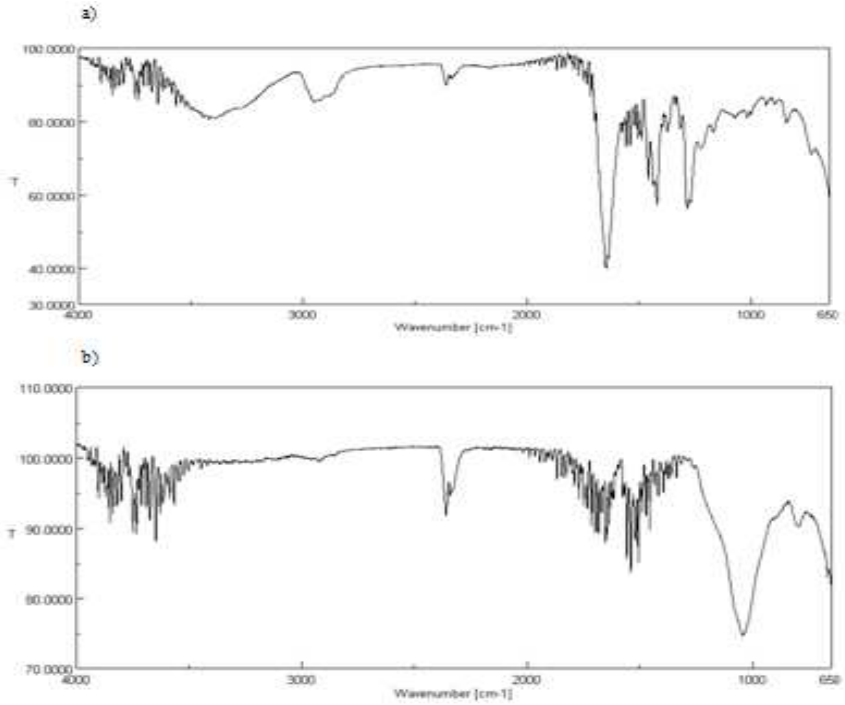

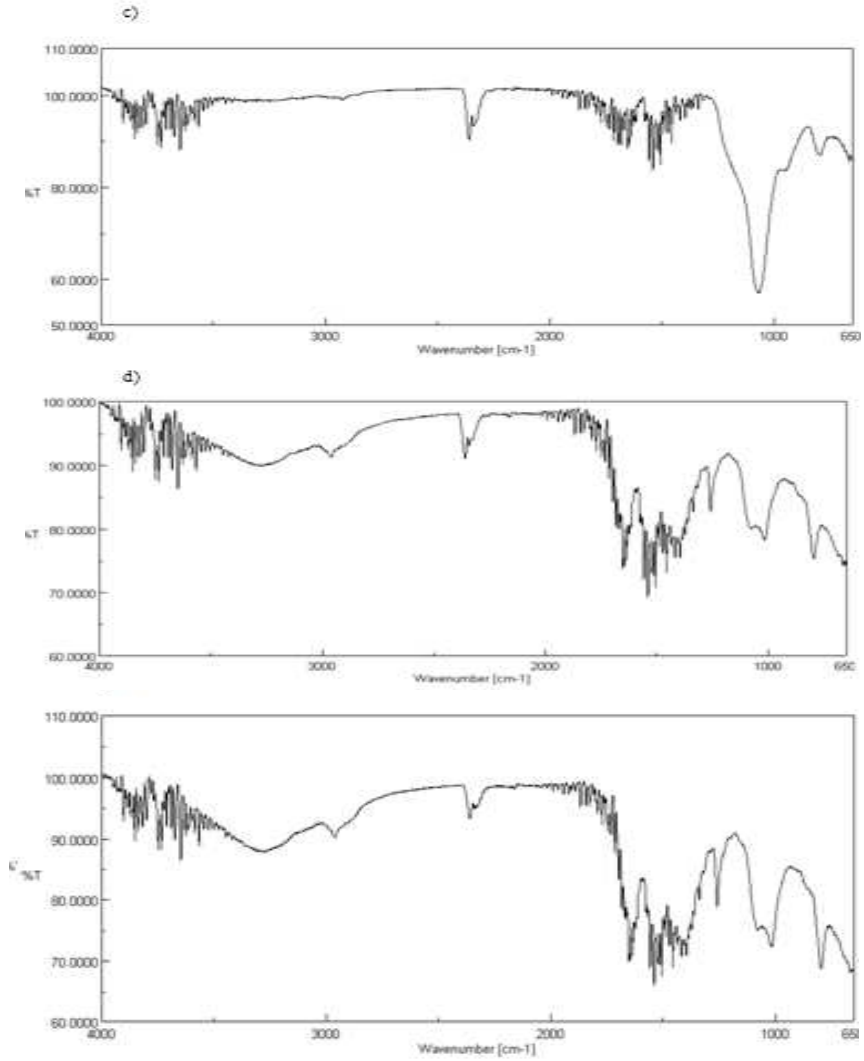

Figure 25: FTIR of a) PVP b) 0.004 mol dm^{-3} TEOS (99.999%) S_1 c) 0.002 mol dm^{-3} TEOS (99.999%) sample 2 d) using gelatin at 100 °C S_3 f) using gelatin at 80 °C sample 4, aged 24 hrs.

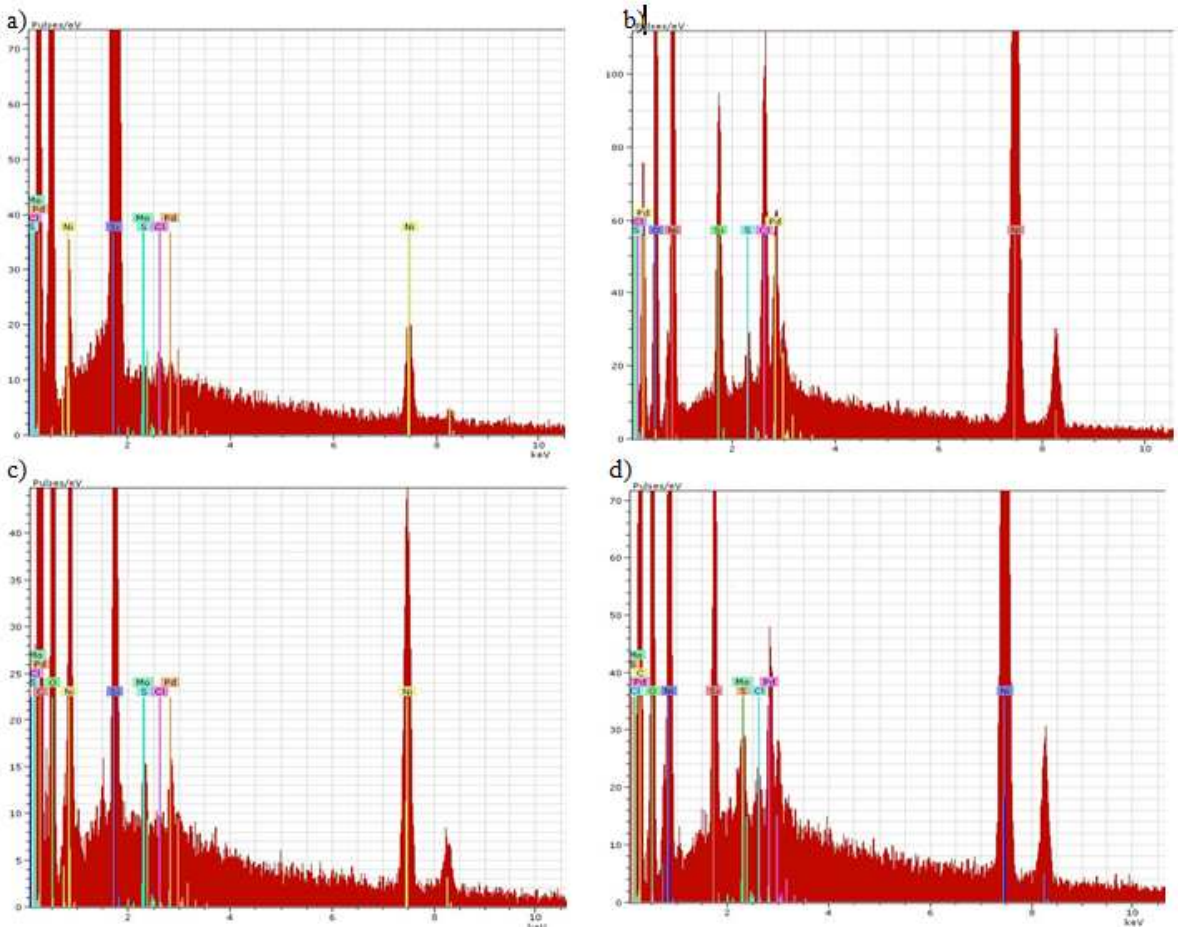

Figure 21: EDX patterns of a) 0.002 mol dm^{-3} TEOS (99.999%) S_2 b) 0.004 mol dm^{-3} TEOS (99.999%) S_1 c) using gelatin at 80 °C S4 d) using gelatin at 100 °C S_3 , aged 24 hrs.

Furthermore, there are no peaks corresponding to crystalline SiO_2 although Si does appear in both EDX (see Fig.26) and FTIR patterns (see Fig.25 b-f). Similar observations have been previously noted [45, 58]. The results denote that the silica structure is amorphous. It is highly unlikely that crystalline silica will be formed at temperatures below 150°C. As consequences from XRD, EDX, FTIR, Ni (Core)/ SiO_2 Shell nanoparticles may possess the structure shown in figure 27.

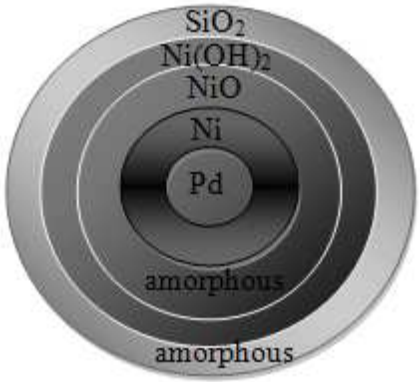

Figure 22: Structure of coating nanoparticles

Role of ageing time: The thickness of shell can be modified by increasing ageing time [46]. By increasing the ageing time, the shell became more organised and smaller. It has been seen from TEM images of S_2, and S_4 (see Fig. 28) that 1 hour is not enough to coat the particles as the formation of the silica shell around the particles is incomplete.

a) **b)**

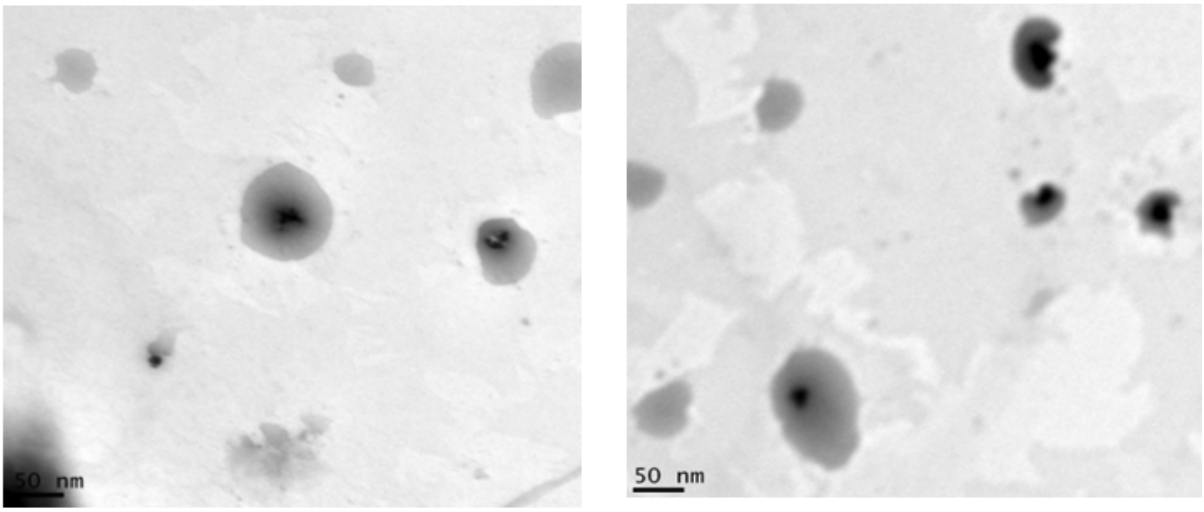

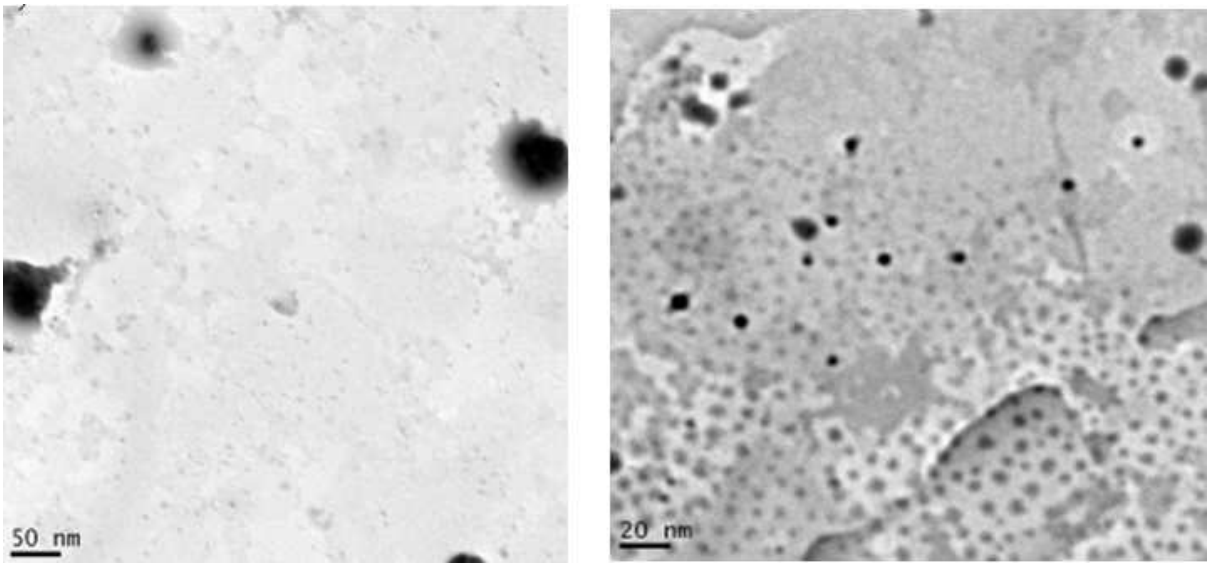

Figure 23: TEM images of diluted samples (10 times) ai) and aii) 0.002 mol dm^{-3} TOES (99.999%) sample 2 bi) and aii) using gelatine at 80c° sample 4, aged 1 hour.

4.4 Conclusions

In this work, Nickel acetate (as precursor), Pd seeds and PVP as stabilizer in situ of propanol-1 were used in the synthesis of Ni magnetic nanoparticles yielding spherical Ni nanocrystals with an average 10 nm. The chemical reaction can be described in the following equations:

$$2.5O_2 + PdCl_2 + C_3H_7OH \rightarrow Pd + 3CO_2 + 3H_2O + 2HCl$$

$$Pd + PVP \rightarrow Pd\text{-}PVP$$

$$8O_2 + Ni(CH3COO)_2 + Pd\text{-}PVP + C_3H_7OH \rightarrow Ni\text{-}Pd\text{-}PVP + 7CO_2 + 7H_2O$$

Ni nanoparticles were characterised by IR spectroscopy, XRD, SEM, EDX and microanalysis and were found to have a composite structure consisting of a mixture of Ni, Pd, $Ni(OH)_2$ phases, NiO which was amorphous. These particles were paramagnetic at room temperature

and underwent a transition to a ferromagnetic state starting at 175 K. Hysteresis loops at 5 K show evidence of exchange bias. Ni nanoparticles were coated with uniform layers of silica (60-80 nm) by different methods. The gelatin was performed to enhance the attachment of silica layer with the core. The size of silica layer becomes smaller (20-44nm). Concentrations of tetraethylorthosilicate (TEOS), together with ageing time, have shown a significant effect on the shell shape and size.

References

1. C.N.R. Rao, P.J.T., G.U. Kulkarni, *Synthesis, Properties and Applications*. 2007: Springer-Verlag Berlin and Heidelberg GmbH & Co. KG.
2. Byrappa, K., S. Ohara, and T. Adschiri, *Nanoparticles synthesis using supercritical fluid technology - towards biomedical applications.* Advanced Drug Delivery Reviews, 2008. **60**(3): p. 299-327.
3. Buffat, P. and J.P. Borel, *Size effect on the melting temperature of gold particles.* Phys. Rev. A FIELD Full Journal Title:Physical Review A: Atomic, Molecular, and Optical Physics, 1976. **13**(6): p. 2287-98.
4. Faraji, M., Y. Yamini, and M. Rezaee, *Magnetic nanoparticles: synthesis, stabilization, functionalization, characterization, and applications.* J. Iran. Chem. Soc. FIELD Full Journal Title:Journal of the Iranian Chemical Society, 2010. **7**(1): p. 1-37.
5. Lu, A.H., E.L. Salabas, and F. Schueth, *Magnetic nanoparticles: synthesis, protection, functionalization, and application.* Angew. Chem., Int. Ed. FIELD Full Journal Title:Angewandte Chemie, International Edition, 2007. **46**(8): p. 1222-1244.
6. Liu, C., et al., *Oxidation of FePt nanoparticles.* J. Magn. Magn. Mater., 2003. **266**(1-2): p. 96-101.
7. Jeong, U., et al., *Superparamagnetic colloids: controlled synthesis and niche applications.* Adv. Mater. (Weinheim, Ger.) FIELD Full Journal Title:Advanced Materials (Weinheim, Germany), 2007. **19**(1): p. 33-60.
8. Sergey P. Gubin, *Magnetic Nanoparticles*. 2009: Wiley VCH
9. Skumryev, V., et al., *Beating the superparamagnetic limit with exchange bias.* Nature (London, U. K.) FIELD Full Journal Title:Nature (London, United Kingdom), 2003. **423**(6942): p. 850-853.
10. Johnston-Peck Aaron, C., J. Wang, and B. Tracy Joseph, *Synthesis and structural and magnetic characterization of Ni(core)/NiO(shell) nanoparticles.* ACS Nano FIELD Full Journal Title:ACS nano, 2009. **3**(5): p. 1077-84.
11. Yan, J.-M., et al., *Synthesis of Longtime Water/Air-Stable Ni Nanoparticles and Their High Catalytic Activity for Hydrolysis of Ammonia-Borane for Hydrogen Generation.* Inorg. Chem. (Washington, DC, U. S.) FIELD Full Journal Title:Inorganic Chemistry (Washington, DC, United States), 2009. **48**(15): p. 7389-7393.
12. Guo, D., et al., *Study on the enhanced cellular uptake effect of daunorubicin on leukemia cells mediated via functionalized nickel nanoparticles.* Biomed. Mater. (Bristol, U. K.) FIELD Full Journal Title:Biomedical Materials (Bristol, United Kingdom), 2009. **4**(2): p. 025013/1-025013/8.
13. Guo, D., et al., *Synergistic effect of functionalized nickel nanoparticles and quercetin on inhibition of the SMMC-7721 cells proliferation.* Nanoscale Res. Lett. FIELD Full Journal Title:Nanoscale Research Letters, 2009. **4**(12): p. 1395-1402.
14. Guo, D.D., et al., *Electrochemical study of the effect of functionalized nickel nanoparticles on cellular uptake of leukemia cancer cells in vitro.* Chin. Chem. Lett. FIELD Full Journal Title:Chinese Chemical Letters, 2008. **19**(5): p. 577-580.
15. Lee, I.S., et al., *Ni/NiO Core/Shell Nanoparticles for Selective Binding and Magnetic Separation of Histidine-Tagged Proteins.* J. Am. Chem. Soc. FIELD Full Journal Title:Journal of the American Chemical Society, 2006. **128**(33): p. 10658-10659.
16. Gubin, S.P., et al., *Magnetic nanoparticles: Preparation, structure and properties.* Russ. Chem. Rev. FIELD Full Journal Title:Russian Chemical Reviews, 2005. **74**(6): p. 489-520.

17. Hou, Y., et al., *Size-controlled synthesis of nickel nanoparticles.* Appl. Surf. Sci. FIELD Full Journal Title:Applied Surface Science, 2005. **241**(1-2): p. 218-222.
18. De Caro, D. and J.S. Bradley, *Surface Spectroscopic Study of Carbon Monoxide Adsorption on Nanoscale Nickel Colloids Prepared from a Zerovalent Organometallic Precursor.* Langmuir FIELD Full Journal Title:Langmuir, 1997. **13**(12): p. 3067-3069.
19. Ely, T.O., et al., *Synthesis of Nickel Nanoparticles. Influence of Aggregation Induced by Modification of Poly(vinylpyrrolidone) Chain Length on Their Magnetic Properties.* Chem. Mater. FIELD Full Journal Title:Chemistry of Materials, 1999. **11**(3): p. 526-529.
20. Luo, X., et al., *Preparation of hexagonal close-packed nickel nanoparticles via a thermal decomposition approach using nickel acetate tetrahydrate as a precursor.* J. Alloys Compd. FIELD Full Journal Title:Journal of Alloys and Compounds, 2009. **476**(1-2): p. 864-868.
21. Davar, F., Z. Fereshteh, and M. Salavati-Niasari, *Nanoparticles Ni and NiO: Synthesis, characterization and magnetic properties.* J. Alloys Compd. FIELD Full Journal Title:Journal of Alloys and Compounds, 2009. **476**(1-2): p. 797-801.
22. Frey, N.A., et al., *Magnetic nanoparticles: synthesis, functionalization, and applications in bioimaging and magnetic energy storage.* Chem. Soc. Rev. FIELD Full Journal Title:Chemical Society Reviews, 2009. **38**(9): p. 2532-2542.
23. Green, M. and P. O'Brien, *The preparation of organically functionalized chromium and nickel nanoparticles.* Chem Commun (Camb) FIELD Full Journal Title:Chemical communications (Cambridge, England), 2001(19): p. 1912-3.
24. Hou, Y. and S. Gao, *Monodisperse nickel nanoparticles prepared from a monosurfactant system and their magnetic properties.* J. Mater. Chem. FIELD Full Journal Title:Journal of Materials Chemistry, 2003. **13**(7): p. 1510-1512.
25. Illy, S., et al., *First direct evidence of size-dependent structural transition in nanosized nickel particles.* Philos. Mag. A FIELD Full Journal Title:Philosophical Magazine A: Physics of Condensed Matter: Structure, Defects and Mechanical Properties, 1999. **79**(5): p. 1021-1031.
26. Teranishi, T. and M. Miyake, *Novel synthesis of monodispersed Pd/Ni nanoparticles.* Chem. Mater. FIELD Full Journal Title:Chemistry of Materials, 1999. **11**(12): p. 3414-3416.
27. Hinotsu, T., et al., *Size and structure control of magnetic nanoparticles by using a modified polyol process.* J. Appl. Phys. FIELD Full Journal Title:Journal of Applied Physics, 2004. **95**(11, Pt. 2): p. 7477-7479.
28. Y. Bahari Mollamahale, D.H., S. K. Sadrnezhaad. *Surfactant-Free Nonaqueous Route for Preparation of Metallic Nickel Nanoparticles*. in *Proceedings of the 3rd Conference on Nanostructures (NS2010)*. 2010. Kish Island, I.R. Iran.
29. Alonso, F., et al., *Preparation of nickel(0) nanoparticles by arene-catalysed reduction of different nickel chloride-containing systems.* J. Exp. Nanosci. FIELD Full Journal Title:Journal of Experimental Nanoscience, 2006. **1**(1-4): p. 419-433.
30. Alonso, F., et al., *Nickel nanoparticles in hydrogen-transfer reductions: Characterisation and nature of the catalyst.* Appl. Catal., A FIELD Full Journal Title:Applied Catalysis, A: General. **378**(1): p. 42-51.
31. Chen, D.-H. and C.-H. Hsieh, *Synthesis of nickel nanoparticles in aqueous cationic surfactant solutions.* J. Mater. Chem. FIELD Full Journal Title:Journal of Materials Chemistry, 2002. **12**(8): p. 2412-2415.
32. Wang, H., et al., *Large scale synthesis and characterization of Ni nanoparticles by solution reduction method.* Bull. Mater. Sci. FIELD Full Journal Title:Bulletin of Materials Science, 2008. **31**(1): p. 97-100.
33. Wu, S.-H. and D.-H. Chen, *Synthesis and stabilization of Ni nanoparticles in a pure aqueous CTAB solution.* Chem. Lett. FIELD Full Journal Title:Chemistry Letters, 2004. **33**(4): p. 406-407.
34. Gong, J., et al., *Structural and magnetic properties of hcp and fcc Ni nanoparticles.* J. Alloys Compd. FIELD Full Journal Title:Journal of Alloys and Compounds, 2008. **457**(1-2): p. 6-9.
35. Scherer, C.J.B.G.W., *Sol-Gel Science: The Physics and Chemistry of Sol-Gel Processing*

1 edition ed. 1990: Academic Press; .
36. Yang, J., et al., *Synthesis and magnetic properties of Mg-doped hexagonal close-packed Ni nanoparticles.* J. Alloys Compd. FIELD Full Journal Title:Journal of Alloys and Compounds, 2009. **467**(1-2): p. L21-L25.
37. Wei, Z., et al., *Microstructural characterization of Ni nanoparticles prepared by anodic arc plasma.* Mater. Charact. FIELD Full Journal Title:Materials Characterization, 2006. **57**(3): p. 176-181.
38. Chang, H. and H.-T. Su, *Synthesis and magnetic properties of Ni nanoparticles.* Rev. Adv. Mater. Sci. FIELD Full Journal Title:Reviews on Advanced Materials Science, 2008. **18**(7): p. 669-677.
39. Sue, K., et al., *Synthesis of Ni nanoparticles by reduction of NiO prepared with a flow-through supercritical water method.* Chem. Lett. FIELD Full Journal Title:Chemistry Letters, 2006. **35**(8): p. 960-961.
40. Che, S.L., et al., *Preparation of dense spherical Ni particles and hollow NiO particles by spray pyrolysis.* J. Mater. Sci. FIELD Full Journal Title:Journal of Materials Science, 1999. **34**(6): p. 1313-1318.
41. Lee, Y.-i., et al., *Preparation of nickel nanoparticles in water-in-oil microemulsion.* Diffus. Defect Data, Pt. B FIELD Full Journal Title:Diffusion and Defect Data--Solid State Data, Pt. B: Solid State Phenomena, 2007. **124-126**(Pt. 2, Advances in Nanomaterials and Processing, Part 2): p. 1193-1196.
42. Chen, D.-H. and S.-H. Wu, *Synthesis of Nickel Nanoparticles in Water-in-Oil Microemulsions.* Chem. Mater. FIELD Full Journal Title:Chemistry of Materials, 2000. **12**(5): p. 1354-1360.
43. Nagaveni, K., et al., *Pd-coated Ni nanoparticles by the polyol method: an efficient hydrogenation catalyst.* J. Mater. Chem. FIELD Full Journal Title:Journal of Materials Chemistry, 2002. **12**(10): p. 3147-3151.
44. Lu, P., et al., *Polymer-Protected Ni/Pd Bimetallic Nano-Clusters: Preparation, Characterization and Catalysis for Hydrogenation of Nitrobenzene.* J. Phys. Chem. B FIELD Full Journal Title:Journal of Physical Chemistry B, 1999. **103**(44): p. 9673-9682.
45. Tang, N., et al., *Synthesis and magnetic properties of carbon-coated Ni/SiO2 core/shell nanocomposites.* Sci. China, Ser. G: Phys., Mech. Astron. FIELD Full Journal Title:Science in China, Series G: Physics, Mechanics & Astronomy, 2009. **52**(1): p. 31-34.
46. Ohmori, M. and E. Matijevic, *Preparation and properties of uniform coated colloidal particles. VII. Silica on hematite.* J. Colloid Interface Sci. FIELD Full Journal Title:Journal of Colloid and Interface Science, 1992. **150**(2): p. 594-8.
47. Wang, G. and A. Harrison, *Preparation of Iron Particles Coated with Silica.* J. Colloid Interface Sci. FIELD Full Journal Title:Journal of Colloid and Interface Science, 1999. **217**(1): p. 203-207.
48. Graf, C., et al., *A General Method To Coat Colloidal Particles with Silica.* Langmuir FIELD Full Journal Title:Langmuir, 2003. **19**(17): p. 6693-6700.
49. Khoshhesab, Z.M. and M. Sarfaraz, *Preparation and Characterization of NiO Nanoparticles by Chemical Precipitation Method.* Synth. React. Inorg., Met.-Org., Nano-Met. Chem. FIELD Full Journal Title:Synthesis and Reactivity in Inorganic, Metal-Organic, and Nano-Metal Chemistry, 2010. **40**(9): p. 700-703.
50. Qiao, H., et al., *Preparation and characterization of NiO nanoparticles by anodic arc plasma method.* J. Nanomater. FIELD Full Journal Title:Journal of Nanomaterials, 2009: p. No pp given.
51. Khoshhesab, Z.M. and M. Sarfaraz, *Preparation and Characterization of NiO Nanoparticles by Chemical Precipitation Method.* Synth. React. Inorg., Met.-Org., Nano-Met. Chem. FIELD Full Journal Title:Synthesis and Reactivity in Inorganic, Metal-Organic, and Nano-Metal Chemistry. **40**(9): p. 700-703.

52. Li, Z., et al., *Preparation of polyvinylpyrrolidone-protected Prussian blue nanocomposites in microemulsion.* Colloids Surf., A FIELD Full Journal Title:Colloids and Surfaces, A: Physicochemical and Engineering Aspects, 2004. **243**(1-3): p. 63-66.
53. Chen, X. and Y. Lin, *Photochromism of Peroxotungstic Acid/PVP Nanocomposite Obtained by Sol-Gel Method.* J. Sol-Gel Sci. Technol. FIELD Full Journal Title:Journal of Sol-Gel Science and Technology, 2005. **36**(2): p. 197-201.
54. Tu, W.-x., X.-b. Zuo, and H.-f. Liu, *Study on the interaction between polyvinylpyrrolidone and platinum metals during the formation of the colloidal metal nanoparticles.* Chin. J. Polym. Sci. FIELD Full Journal Title:Chinese Journal of Polymer Science, 2008. **26**(1): p. 23-29.
55. Lu, X., et al., *Superdispersible PVP-Coated Fe3O4 Nanocrystals Prepared by a "One-Pot" Reaction.* J. Phys. Chem. B FIELD Full Journal Title:Journal of Physical Chemistry B, 2008. **112**(46): p. 14390-14394.
56. Couto, G.G., et al., *Nickel nanoparticles obtained by a modified polyol process: Synthesis, characterization, and magnetic properties.* J. Colloid Interface Sci. FIELD Full Journal Title:Journal of Colloid and Interface Science, 2007. **311**(2): p. 461-468.
57. Xie, A., et al., *Coordination and phase separation in polyvinylpyrrolidone-neodymium chloride complex.* J. Mater. Sci. Lett. FIELD Full Journal Title:Journal of Materials Science Letters, 2002. **21**(4): p. 345-347.
58. Tang, N.J., et al., *Synthesis and complex permeability of Co/SiO2 nanocomposites.* Mater. Lett. FIELD Full Journal Title:Materials Letters, 2005. **59**(14-15): p. 1723-1726.